Carruthers Vernon B (Orcid ID: 0000-0001-6859-8895)

Original Research
TRA.12556
doi: 10.1111/TRA.12556
Society number TRA-17-0683
NIH funded YES
Manuscript received 20 October 2017
Revised and accepted 10 February 2018
Sent to press 10 February 2018
Color figures: 1, 2, 3, 4, 5, 6, 7, 8
Supp Mat: 1, 2, 3, 4, 5
Synopsis included YES
Abstract figure included YES
Editorial process file included YES

Intersection of Endocytic and Exocytic Systems in *Toxoplasma gondii*

Olivia L. McGovern, Yolanda Rivera-Cuevas, Geetha Kannan, Andrew Narwold Jr., and Vern B. Carruthers

Department of Microbiology and Immunology, University of Michigan School of Medicine, Ann Arbor, MI USA 48109-5620

Corresponding author:
Vern Carruthers
Department of Microbiology and Immunology, University of Michigan School of Medicine, 1150 W Medical Center Drive, 5740 Medical Science Building II, Ann Arbor, MI USA 48109-5620
Phone: 734-763-2081, Fax: 734-764-3562, Email: vcarruth@umich.edu

RUNNING TITLE
T. gondii endo- and exocytic trafficking intersect

KEYWORDS
Toxoplasma gondii, endocytosis, ingestion, exocytosis, microneme, rhoptry, intracellular trafficking

SYNOPSIS

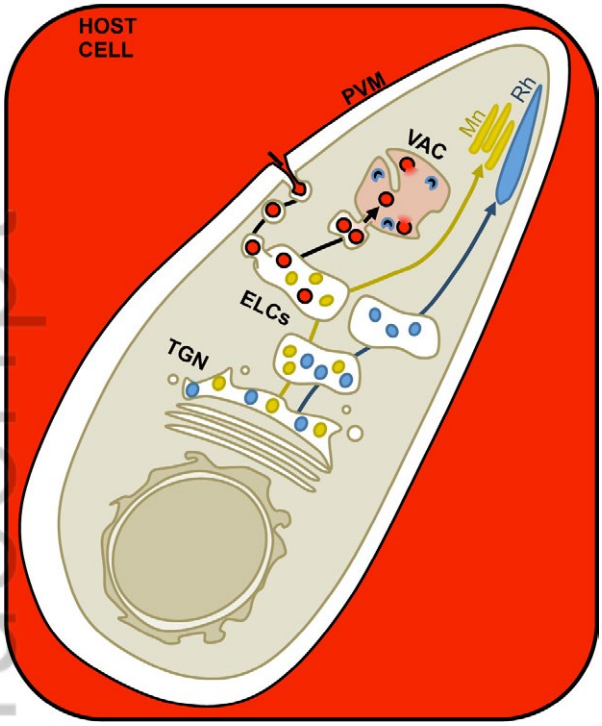

The dynamics and route of *T. gondii* endocytic trafficking are undefined. We show host proteins are endocytosed across the parasitophorous vacuole membrane (PVM) within 7 minutes post-invasion, trafficked in a TgDrpB-independent manner through endosome-like compartments, and are delivered to the parasite's lysosome-like compartment (VAC) for degradation within 30 minutes. Endocytic trafficking occurs simultaneously with exocytic trafficking to the parasite's regulated secretory organelles, micronemes (Mn) and rhoptries (Rh), but intersects with microneme trafficking only. endosome-like compartments; ELC.

ABSTRACT

Host cytosolic proteins are endocytosed by *Toxoplasma gondii* and degraded in its lysosome-like compartment, the VAC, but the dynamics and route of endocytic trafficking remain undefined. Conserved endocytic components and plant-like features suggest *T. gondii* endocytic trafficking involves transit through early and late endosome-like compartments (ELCs) and potentially the trans-Golgi network (TGN) as in plants. However, exocytic trafficking to regulated secretory organelles, micronemes and rhoptries, also proceeds through ELCs and requires classical endocytic components including a dynamin-related protein, DrpB. Here we show that host cytosolic proteins are endocytosed within 7 min post-invasion, trafficked through ELCs en route to the VAC, and degraded within 30 min. We could not definitively interpret if ingested protein is trafficked through the TGN. We also found that parasites ingest material from the host cytosol throughout the parasite cell cycle. Ingested host proteins colocalize with immature microneme proteins, proM2AP and proMIC5, in transit to the micronemes, but not with the immature rhoptry protein proRON4, indicating that endocytic trafficking of ingested protein intersects with exocytic trafficking of microneme proteins. Finally, we show that conditional expression of a DrpB dominant negative mutant increases *T. gondii* ingestion of host-derived proteins, suggesting that DrpB is not required for parasite endocytosis.

INTRODUCTION

Toxoplasma gondii is a eukaryotic, obligate intracellular parasite that resides within a membrane compartment called the parasitophorous vacuole (PV). *T. gondii* belongs to the phylum Apicomplexa, which also includes other notable human pathogens such as *Plasmodium*, the causative agents of human malaria. While *T. gondii* infection of immunocompetent individuals usually results in mild flu-like symptoms, reactivated chronic infection in immunocompromised individuals or congenital infection through vertical transmission can be life threatening, produce symptoms similar to septic shock and potentially leading to vision loss.[1, 2] Toxoplasmosis is believed to be lifelong and is currently incurable, leaving the two billion people chronically infected worldwide susceptible to the consequences of reactivated toxoplasmosis.[1, 2] Therefore, a better understanding of the fundamental features of infection is needed to uncover new treatment options and limit the burden of toxoplasmosis.

One of the most central and necessary aspects of life for a eukaryotic cell is endocytosis. Endocytosis is pathway by which material is taken up across the plasma membrane and trafficked to the lysosome for digestion. An analogous pathway was recently discovered in *T. gondii* termed the ingestion pathway. In *T. gondii* ingestion, proteins acquired from the host cell cytosol are trafficked across the PV and parasite plasma membrane to a lysosome-like compartment within the parasite termed the vacuolar compartment/plant-like vacuole (VAC/PLV; the term VAC will be used hereafter) for degradation.[3] The ability to deliver host cytosol and/or parasite-derived material to the VAC for digestion contributes to the acute stage infection and is especially important for chronic infection.[3, 4] However, how ingested cargoes are delivered to the VAC is not known.

Endocytic trafficking to the lysosome is highly conserved among eukaryotes with a slight variation observed in plants. In mammalian and yeast cells, endocytic cargoes are delivered sequentially to the Rab5 compartment, the Rab7 compartment and finally to the lysosome.[5] Plant cells, on the other hand, initially deliver endocytosed cargoes to the trans-Golgi network (TGN), followed by sequential movement through the Rab5 compartment, the Rab7 compartment and finally the lysosome for degradation.[6] *Toxoplasma* has a conserved endomembrane structure including a TGN, endosome-like compartments (ELCs) marked by Rab5 and Rab7, and the lysosome-like VAC, and also expresses the essential machinery for endocytic trafficking to lysosomes including clathrin, dynamin, Rab5 and Rab7.[7] The presence of a plant-like lysosome and a plant-specific proton pump (TgVP1) within the *T. gondii* endolysosomal system[8] suggests that endocytic trafficking in *T. gondii* may resemble plants as proposed by *Pieperhoff et al.*[9] However, exocytic trafficking of proteins destined for the parasite's regulated secretory organelles, the micronemes and rhoptries, proceeds through the TGN and ELCs, and requires clathrin, dynamin and Rab5 for transit.[9-16] In contrast to the ingestion pathway, which leads to the destruction of its cargo, most microneme and rhoptry proteins have propeptides that are cleaved off during transit to the microneme and rhoptry organelles, but must otherwise remain intact to orchestrate parasite invasion, egress and defense against host immune attack.[17-27] Without these exocytic proteins and organelles, the parasite cannot establish a successful infection.

How *T. gondii* ensures proper targeting of endocytic and exocytic cargo is unclear, but other eukaryotic systems reveal several possible mechanisms. Endocytic and exocytic trafficking may be spatially regulated like certain GPI-anchored proteins that traffic directly to the plasma membrane from the TGN, avoiding endosomes in mammalian cells.[28] Alternatively, these processes may be temporally regulated. In *Plasmodium spp.*, endocytosis of red blood cell cytoplasm is most active in G1 and early S phase, whereas microneme organelle biogenesis occurs later in the late S and mitosis and cytokinesis (M/C) phases.[29-33] Another scenario is that endocytic and exocytic trafficking intersect and require sorting mechanisms to ensure proper targeting. This is illustrated by the TGN in plants, which serves as a sorting station for endocytic and exocytic cargoes, or by transferrin receptors in mammalian cells, which traffic through endosomes before reaching the plasma membrane.[28, 34]

In this study, we determined temporal and spatial relationships between endocytic and exocytic trafficking within *T. gondii* and investigated the role of the dynamin-related protein DrpB in endocytic trafficking. We find that host cytosolic proteins are ingested during or immediately following invasion, are trafficked through ELCs, and delivered to the VAC for degradation in 30 min. Ingestion and immature promicroneme proteins can be detected in all phases of the cell cycle, whereas immature prorhoptry protein detection is restricted to the S and M/C phases. Further, ingested proteins colocalize with promicroneme, but not prorhoptry proteins, suggesting endocytic trafficking of ingested protein intersects with exocytic trafficking of microneme proteins. Finally, endocytic trafficking of ingested protein does not require DrpB, but may require a DrpB binding partner.

RESULTS

Localization of TGN/ELC markers: GalNac and DrpB

Plant-like features of *T. gondii* led to the prediction that ingested proteins follow a plant-like endocytic route through the TGN and ELCs en route to the VAC. To test if the endocytic trafficking is plant-like in *T. gondii*, we generated a parasite line stably expressing UDP-GalNAc:polypetide N-acetylgalactosaminyl-transferase fused to YFP (GalNac-YFP), typically used as a TGN marker.[35] Consistent with TGN localization, GalNac-YFP appeared in a centrally located structure that overlapped substantially with, or was just apical to, the Golgi marker GRASP55-mRFP (Figure S1). As previously observed, GalNac-YFP sometimes showed a high degree of overlap with another TGN marker the dynamin-related protein DrpB (Figure S1A top panel), but in other cases showed partial or no overlap with DrpB (Figure S1A bottom panel). Interestingly, GalNac-YFP

overlapped best with NHE3 in the central region of the parasite despite previous observations that NHE3 partially colocalized with the VAC.[36] Therefore, we interpret NHE3 to be an ELC marker that partially overlaps with the TGN, similar to the established ELC marker proM2AP.[10, 37] GalNac-YFP also partially overlapped with proM2AP, but rarely colocalized with the VAC markers CPB and CPL or the apicoplast. We also observed that some parasites had GalNac-YFP-labeled structures that were not associated with GRASP55-mRFP (Figure S1, white arrowheads). These structures are reminiscent of "Golgi-free" TGN bodies in plants[38] This observation together with substantial overlap with the ELC marker proM2AP, suggests GalNac-YFP occupies the TGN, ELCs, and perhaps additional sites.

To visualize DrpB as a second marker of the TGN we utilized the RHΔhx ddFKBP-GFP-DrpB WT (ddGFP-DrpB WT) strain.[12] These parasites express an ectopic copy of DrpB fused to GFP and a destabilization domain (dd), which allows for post-translational control of protein expression upon adding the stabilizing drug Shield-1. To minimize possible off-target effects due to DrpB overexpression, Shield-1 treatment was optimized to observe ddGFP-DrpB WT expression in the majority of parasites with minimal treatment: 0.8μM Shield-1 for 30 min. Under these conditions, ddGFP-DrpB WT overexpression did not interfere with microneme trafficking as previously observed (Figure S2A and B).[12] As shown in Figure S1, DrpB localization was slightly different from that of GalNac-YFP. ddGFP-DrpB WT showed little to no overlap with the VAC marker CPL, but colocalized most prominently with proM2AP and only partially overlapped with NHE3 (Figure S2C top panels). This localization was confirmed by staining of endogenous DrpB with a DrpB antibody, suggesting overexpression under these conditions also did not cause mislocalization of ddGFP-DrpB WT (Figure S2C bottom panels). Taken together, these findings suggest that ddGFP-DrpB WT may also localize to both the TGN and ELCs.

Ingested proteins traverse ELCs

The ability of *T. gondii* to ingest proteins from the host cytosol can be monitored using fluorescent protein reporters such as mCherry (Figure 1A). Chinese hamster ovary (CHO-K1) cells transiently transfected with a plasmid encoding cytosolic mCherry are infected with *T. gondii* and incubated to allow consumption of host cytosol. Parasites are then purified from host cells and analyzed by fluorescence microscopy. In our previous study, accumulation of ingested host protein was enhanced by the absence of the VAC-localized protease CPL or by treatment with a CPL inhibitor, morpholinurea-leucine-homophenylalanine-vinyl phenyl sulfone (LHVS).[3] mCherry$^+$ parasites are capable of invading new host cells, indicating that these parasites are viable (Figure S3A-C). When LHVS-dependent accumulation of ingested host protein ingestion is detected, the ingestion pathway is considered to be active, and the percentage of ingested mCherry puncta overlapping with endolysosomal system markers (%Colocalized) can be determined as a measure of localiztion.

To determine which endolysosomal compartments ingested protein traffics through on the way to the VAC, GalNac-YFP, WT (RH), or ddGFP-DrpB WT parasites were treated and processed as shown in Figure 1A with the addition of Shield-1 treatment to induce stabilization of ddGFP-DrpB WT, and stained with antibodies against proM2AP, NHE3, or CPB. As a negative control, the apicoplast, a compartment that is in the same region as, but distinct from, the endolysosomal system, was stained with DAPI as a test for random colocalization. Ingestion was found to be active in all three strains, and Shield-1 treatment of ddGFP-DrpB WT parasites did not affect ingestion (Figure 1B-D). Localization analysis in these parasites revealed that ingested protein significantly colocalized with GalNac-YFP, ddGFP-DrpB WT, proM2AP and CPB, but not NHE3 when compared to the apicoplast (Figure 1E and F).

Similar levels of colocalization of ingested protein with ddGFP-DrpB WT and proM2AP are expected due to their high degree of overlap (Figure S2C), but why ingested protein colocalized significantly with GalNac-YFP, but not NHE3 despite their near perfect overlap in the central region of the parasite was puzzling. Further investigation revealed that most of the ingested mCherry that colocalized with GalNac-YFP also simultaneously colocalized with CPB (Figure S3D and E). This was not due to redistribution of GalNac-YFP in response to LHVS treatment since overlap of GalNac-YFP with CPB and CPL did not change with treatment (Figure S3F). GalNac-YFP also still showed substantial overlap with NHE3 in the central region of the parasite, and both GalNac-YFP and NHE3 showed only rare overlap with CPB when treated with LHVS (Figure S3G). Further analysis of the GalNac-YFP$^+$CPB$^+$ compartment showed that it is labeled with CPL, proM2AP and NHE3 (Figure S3H), implying it is a subdomain of the ELCs or the VAC rather than the TGN. However, we cannot rule out the possibility that GalNac$^+$CPB$^+$ puncta represent a TGN subcompartment reserved for sorting of both ingested and biosynthetic cargoes to the ELCs and VAC. Although we can clearly distinguish localization of ingested protein from the apicoplast and NHE3 compartment, the dynamic localization of TGN markers within the apical region of the parasite makes their colocalization with ingested protein difficult to definitively interpret. Therefore, we cannot conclusively determine whether ingested proteins are trafficked through the TGN. Nevertheless, the data is consistent with ingested proteins trafficking through ELCs on the way to the VAC.

Ingested proteins reach the VAC for CPL-dependent digestion within 30 min

To better understand the dynamics of ingested protein trafficking to the VAC, GalNac-YFP parasites were treated as shown in Figure 1A, purified at 15 min intervals through the first hour of infection, and LHVS-treated parasites were stained with antibodies against CPB and CPL to label the VAC. Parasite-

associated mCherry was detected at the earliest time point (7 min post-invasion) and throughout the first hour of infection (Figure 2A). Intriguingly, accumulation of mCherry at 7 min post-invasion was independent of LHVS treatment (Figure 2A). Although external protease treatment of purified parasites is routinely performed to remove host protein sticking to the parasite surface, we wanted to ensure the mCherry accumulation was truly inside the parasite. Deconvolution of Z-stack images confirmed that the mCherry accumulation is fully contained within the parasite, and ingested mCherry was resistant to external protease treatment while the parasite surface protein SAG1 was not (Figure S4A and B). These findings suggest host proteins are ingested either during or immediately after invasion and initially delivered into a non-proteolytic compartment.

Detection of ingested mCherry became increasingly dependent on LHVS treatment at 22 min post-invasion and beyond with ingestion in DMSO-treated parasites reaching the typically observed basal levels by 37 min post-invasion (Figure 2A). Colocalization of ingested mCherry with CPB/L increases as detection of ingested protein in DMSO-treated parasites decreases, and colocalization with CPB/L peaks at 37 min post-invasion (Figure 2B and C). This suggests that ingested host proteins are trafficked to the VAC and degraded within 30 min. Localization within the GalNac-YFP^{+}CPB/L^{+} compartment also peaked at 37 min post-invasion (Figure S4C), indicating that this compartment is digestive in nature, further supporting its identity as a subdomain of the ELCs or the VAC.

Promicroneme proteins are detected in all cell cycle phases

Antibody staining against propeptides of microneme and rhoptry proteins label newly synthesized, immature promicroneme and prorhoptry proteins in transit to their respective organelles and possibly also cleaved propeptide, but not mature proteins in the microneme and rhoptry organelles. For example, staining for the propeptide of the microneme protein M2AP (proM2AP) or rhoptry protein ROP4 (proROP4) shows overlap with the TGN and ELCs but not the micronemes or rhoptries.[10, 16, 37, 39] Therefore, the colocalization of ingested protein with proM2AP noted above suggests that endocytic trafficking to the VAC may intersect with exocytic trafficking to microneme and rhoptry organelles. An important limitation of this experiment, however, is that parasites were treated with LHVS for 36 h prior to infection to emulate detection of ingested host protein in the CPL knockout. Under these conditions, ingested host protein persists with a half-life of 2 to 3 h.[3] Persistent accumulation presumably occurs within the VAC, but trafficking might also be backed up in upstream compartments like the ELCs. Therefore, we cannot differentiate protein ingested several hours ago from actively trafficking, newly ingested protein. So while we conclude that proM2AP and ingested protein are trafficked through the ELCs, this experiment does not conclusively demonstrate that they occupy the ELCs at the same time under normal conditions. Nevertheless, how these cargoes can be trafficked through the same compartment, yet meet very different fates is unclear.

To test if endocytic and exocytic trafficking in *T. gondii* are temporally separated processes, we next sought to determine when during the cell cycle microneme or rhoptry biogenesis and ingestion occur. *T. gondii* divides by building daughter parasites within the mother cell in a process called endodyogeny and has a cell cycle characterized by three phases: G, S, M/C.[40] Progression through the *T. gondii* cell cycle can be monitored using two markers: TgCentrin2 (Cen2) which associates with the centrosome and additional apical structures, and IMC1 which associates with the inner membrane complex and outlines the periphery of the mother cell and newly forming daughter parasites.[41] In the G phase, parasites display a single mother IMC1 structure and a single centrosome. In S phase, the centrosome is duplicated and in M/C phase, two additional U-shaped IMC1 structures outlining the newly forming daughter cells will appear within the IMC1 outline of the mother parasite. To test when microneme or rhoptry biogenesis occurs during the cell cycle, Cen2-EGFP parasites were stained with antibodies against IMC1 to determine cell cycle phase and against propeptides of microneme and rhoptry proteins, which in previous experiments have been associated with timing of microneme and rhoptry biogenesis.[21]

We first examined microneme protein synthesis using antibodies against proM2AP and proMIC5. proM2AP staining has been observed in all phases of the cell cycle, but to what extent remained unclear.[10, 37] Parasites were analyzed at 4 to 6 h post-invasion when parasites in all three phases of the cell cycle were present. proM2AP and proMIC5 were detected in G, S and M/C phases, and in the majority of parasite-containing vacuoles (Figure 3A-D). To ensure that this was not a product of pulse invasion into host cells or only characteristic of the first cell division, asynchronous, overnight cultures of parasites allowed to naturally invade host cells were also analyzed. Again, proM2AP and proMIC5 were detected in G, S and M/C phases and in the majority of parasite-containing vacuoles (Figure 3E-H), suggesting that microneme protein synthesis occurs throughout the cell cycle.

Prorhoptry proteins are detected in S and M/C phases

We next examined detection of rhoptry protein synthesis using antibody staining against proROP4 or proRON4, which is known label M/C phase parasites.[20, 42] The antibody mAb T5 4H1 used to detect proRON4, also detects the moving junction. As previously observed, staining of the moving junction remained on the PVM at 4 to 6 h post-invasion and could not be distinguished from staining within the parasites.[21, 42] Therefore, RON4 synthesis was only analyzed in asynchronous overnight cultures. proROP4 and proRON4 were detected in both S and M/C phases, but were absent from nearly all parasite vacuoles in G phase at 4 to 6 or 24 h post-invasion (Figure 4). This suggests that rhoptry protein synthesis is restricted to later in the cell cycle, and occurs in both S and M/C phases.

Ingestion is active throughout the cell cycle

We next sought to determine when during the cell cycle *T. gondii* ingests host proteins. To more precisely measure when parasites are ingesting protein from the host cell, LHVS treatment was reduced from 36 h to 30 min, adding LHVS immediately prior to parasite purification (Figure 5A). This is the time it takes to complete one ingestion event from uptake to turn over (Figure 2) and should reflect only recently ingested protein. To do this, the LHVS concentration had to be increased from 1 µM to 50 µM, but detection of ingested protein under this condition was indistinguishable from parasites treated with LHVS for 36 h (Figure 5B).

To test when during the cell cycle the ingestion pathway is active, Cen2-EGFP parasites were treated as in Figure 5A, purified at 4 to 6 h post-invasion when all cell cycle phases were observed (Figure 5C), and stained with antibodies against IMC1. Because promicroneme and prorhoptry proteins were detected with similar cell cycle dynamics during the first and subsequent cell division cycles (Figure 3 and 4), cell cycle dependence of ingestion was not analyzed at 24 h post-invasion for comparison. In samples where ingestion was active (Figure 5D), ingestion of mCherry was observed in parasites of all three cell cycle phases (Figure 5E). To determine if ingestion is down regulated in any phase of the cell cycle, the percentage of mCherry positive parasites was also determined in G, S or M/C phase parasites. No significant differences were observed, suggesting that ingestion is equally active during all phases of the cell cycle (Figure 5F).

Ingested host protein trafficking intersects with microneme protein trafficking

Although our results indicate that ingestion, microneme protein synthesis, and rhoptry protein synthesis are active during the same cell cycle phases and traffic through the ELCs, it is still possible that ingested proteins and microneme or rhoptry proteins could avoid interaction. For example, sequential rounds of ingestion and microneme or rhoptry synthesis could occur independent of the cell cycle. To determine if ingestion is down-regulated during microneme or rhoptry synthesis and if their trafficking paths intersect as suggested by our findings in Figure 1, we compared the trafficking of newly ingested protein with that of newly synthesized microneme and rhoptry proteins en route to their respective apical secretory organelles.

To do this, a new cell line developed during the course of this study was used. These cells, termed CHO-K1 inducible mCherry cells (CHO-K1 imCh), produce cytosolic mCherry in response to induction with doxycycline (Figure S5A). mCherry is expressed in 76.0±0.42% of doxycycline-treated CHO-K1 imCh cells compared to 18.6±4.3% of transiently transfected CHO-K1 cells (Figure S5B). Consistent with the broader expression, we observed mCherry in 42.6±8.7% of parasites treated with LHVS for 36 h. Also, ingested mCherry was detected in 16.5±4.1% of parasites treated with LHVS for 30 min, although in this case the LHVS concentration had to be increased to 200 µM to consistently detect LHVS-dependent mCherry accumulation (Figure S5C and D). It should be noted that despite broader expression the mCherry fluorescence intensity of CHO-K1 imCh cells is about 2.8 times lower than transiently transfected CHO-K1 cells (Figure S5B). Thus, results from CHO-K1 imCh cells might still underrepresent the proportion of parasites that are actively ingesting host-derived protein.

To determine if ingestion is down-regulated during microneme or rhoptry biogenesis, parasites were allowed to ingest mCherry from doxycycline-treated CHO-K1 imCh cells and treated with LHVS for 30 min to exclusively detect newly ingested host protein. The parasites were then purified and stained for proM2AP, proMIC5 and proRON4 to detect newly synthesized microneme and rhoptry proteins. We attempted to detect proROP4, but the antibody did not work well in extracellular parasites. In samples where ingestion was active (Figure 6A), the activity of the ingestion pathway during microneme and rhoptry biogenesis was analyzed by determining the percentage of mCherry positive parasites in populations expressing proMIC5 or proRON4 compared to populations of parasites that are negative for each of these markers. This analysis was not performed for proM2AP since 85.9±8.2% of parasites were expressing proM2AP. Ingestion pathway activity was not significantly different in proMIC5^{+} versus proMIC5^{-} or proRON4^{+} versus proRON4^{-} subpopulations, suggesting that ingestion is not down-regulated during microneme or rhoptry biogenesis (Figure 6B and C). Interestingly, even though ingestion is active during microneme and rhoptry biogenesis, ingested protein colocalized with proM2AP and proMIC5, but not proRON4 when compared to the apicoplast negative control (Figure 6D and E). Therefore, endocytic trafficking of ingested host proteins intersects with exocytic trafficking to micronemes, but not to rhoptries, suggesting that rhoptry trafficking may diverge earlier in the endolysosomal system such as the TGN or occupy functionally distinct ELCs.

***T. gondii* ingestion does not require DrpB**

DrpB promotes exocytic trafficking of a subset of microneme and rhoptry proteins, but significant colocalization of ingested protein with DrpB suggests that DrpB could also be involved in endocytic trafficking in *T. gondii.* Dynamins are GTPases best known for their role in fission of endocytic vesicles forming at plasma membrane into the cytosol, but can also promote membrane fission at the TGN, endosomes and mitochondria[43, 44] *T. gondii* DrpB localizes to the TGN and potentially the ELCs, but has not been observed at the parasite plasma membrane.[9, 12] However, given that dynamin-dependent fission of endocytic vesicles at the plasma membrane is conserved in plants, mammals, fungi and other protozoan parasites including *Plasmodium*[43-47], transient populations of DrpB that are difficult to detect by traditional microscopy could promote endocytosis at the plasma membrane similar to the yeast dynamin-like protein Vps1.[46] If this is true, then interfering with DrpB function will inhibit ingestion and

reduce the percentage of mCherry$^+$ parasites. DrpB could also play a role in downstream trafficking of ingested proteins at the ELCs. In this case, interfering with DrpB function will interfere with delivery of ingested protein to the VAC, reducing colocalization of ingested mCherry with VAC markers and potentially preventing its degradation.

To test whether DrpB plays a role in endocytic trafficking, an inducible dominant negative DrpB mutant was expressed to interfere with DrpB function using RHΔhx ddFKBP-GFP-DrpB K72A (ddGFP-DrpB K72A) parasites. Parasites treated with the vehicle control ethanol are essentially wildtype, but addition of Shield-1 stabilizes ddGFP-DrpB K72A, a GTPase mutant shown to interfere with dynamin function in endocytosis in other organisms.[48] Prolonged, overnight treatment with Shield-1 in this strain leads to aberrant secretion of microneme and rhoptry proteins such as MIC3 into the PV lumen, depletion of microneme and rhoptry organelles and non-invasive parasites.[12] To avoid issues with invasion for the ingestion assay, Shield-1 treatment was optimized to induce dominant negative effects in short periods of time. A significant percentage of vacuoles were positive for MIC3 staining in the PV lumen within 3 but not 2 h of 1μM Shield-1 treatment when compared to the vehicle ethanol-treated control (Figure 7 A and B). Therefore, ingestion assays were performed with ddGFP-DrpB K72A parasites as in Figure 6 with 30 min LHVS treatment to observe recently ingested protein and Shield-1 treatment for up to 3 h to induce expression of ddGFP-DrpB K72A. Following harvest and fixation, parasites were stained with antibodies against proM2AP and CPL or DAPI to label the apicoplast, and the percentage of mCherry$^+$ parasites and localization of ingested mCherry was determined.

ddGFP-DrpB K72A parasites treated with LHVS and ethanol (vehicle for Shield-1) accumulated mCherry, confirming that ingestion is active in this parasite strain (Figure 7C). Interestingly, parasites treated with LHVS and Shield-1 showed a significant increase in the percentage of mCherry$^+$ parasites compared to those treated with LHVS and ethanol (Figure 7C). A similar increase was not observed in DMSO-treated ddGFP-DrpB K72A parasites or in wildtype RH parasites treated with Shield-1, suggesting the increased accumulation of ingested protein was not due to defects in the turnover of ingested protein or off-target effects of Shield-1 itself (Figure 7C and D). Taken together, this suggests that DrpB is not required for fission of endocytic vesicles at the plasma membrane, but may indirectly restrict the rate of ingested protein endocytosis.

Normal turnover of ingested mCherry in parasites treated with DMSO and Shield-1 also suggested that the mCherry was being delivered to the VAC. To confirm this, the localization of ingested mCherry was determined. As previously observed, ingested mCherry showed significant colocalization with proM2AP and CPL when compared to the apicoplast in ethanol-treated control samples (Figure 7E). When comparing ethanol and Shield-1-treated parasites, colocalization of ingested mCherry with proM2AP and the apicoplast was not affected, but surprisingly colocalization with the VAC marker CPL was significantly increased (Figure 7E). Localization of CPL relative to NHE3, proM2AP and CPB and the staining pattern of these markers was not altered under the same Shield-1 treatment conditions, excluding the possibility that increased colocalization with ingested mCherry was due to redistribution of CPL into multiple endocytic compartments, e.g. the VAC and ELCs (Figure 7F-H). Taken together, this suggests that DrpB is also not required for downstream endocytic trafficking of ingested protein to the VAC or trafficking of CPL. Consistent with this, ddGFP-DrpB K72A showed almost no association with the endolysosomal system, maintaining reduced but significant localization with proM2AP, but not NHE3, and was not significantly associated with ingested mCherry or CPL (Figure 7E and G-I). This suggests that ddGFP-DrpB K72A may indirectly increase colocalization between ingested mCherry and CPL, potentially through enhancing the rate of endocytic trafficking to the VAC. Proposed mechanisms for these observations are discussed below. These results also provide functional distinction between exocytic and endocytic trafficking in *T. gondii*, with DrpB likely being devoted to exocytic trafficking only.

DISCUSSION

Trafficking of Ingested Proteins

Our data are consistent with ingested proteins trafficking through the ELCs on the way to the VAC, however we could not conclusively determine if ingested protein is trafficked through the TGN due to extensive localization of GalNac–YFP and ddGFP-DrpB WT with ELC markers. Additionally, ingested protein colocalized with GalNac-YFP in a compartment that predominantly labeled with CPB and CPL and seems to be digestive in nature. This suggests an ELC or VAC-like identity for the GalNac-YFP$^+$CPB/L$^+$ compartment. Indeed, digestion of ingested proteins in prelysosomal compartments has been described in *Plasmodium* parasites. Haemozoin, a visible byproduct of hemoglobin digestion has been observed in transport vesicles en route to the lysosome-like organelle of *Plasmodium* called the digestive vacuole, suggesting that hemoglobin digestion begins and may even be complete before reaching the digestive vacuole.[32, 49] Where digestion begins in *T. gondii* is unclear, but rapid digestion beginning soon after ingestion could explain why very few parasites have detectable levels of ingested protein in the absence of LHVS. Future use of super resolution microscopy and more precise endomembrane markers, especially of the TGN, will better define the localization of ingested protein. Finally, identifying a method for monitoring *T. gondii* ingestion using live-cell imaging will also be invaluable to determine the order that ingested proteins travel through the endolysosomal compartments, the rate of endocytosis, and whether every parasite undergoes endocytosis.

Cell Cycle Dependence of Microneme and Rhoptry Biogenesis

Population-based transcriptomic studies and live cell imaging of fluorescently-tagged microneme and rhoptry proteins suggest

that microneme and rhoptry organelles are made de novo during daughter cell formation once per cell cycle in M/C phase.[50, 51] However, transcript levels do not necessarily correspond to protein levels, and fluorescent tagging of microneme and rhoptry proteins will label both immature protein in transit and mature protein within the microneme and rhoptry organelles. Our data suggests that microneme proproteins are present in all phases of the cell cycle, whereas expression of rhoptry proproteins is limited to S and M/C phase. It should be noted that antibodies used for this study may detect cleaved propeptides, which could persist after mature microneme and rhoptry proteins are further trafficked with an unknown half-life. However, the pattern of protein expression that we observe mirrors expression patterns in transcriptomic data. Microneme transcript levels undulate, but remain high throughout the cell cycle, whereas rhoptry protein transcripts show a much sharper drop in the G phase.[50] Previous work found that expression of promicroneme and prorhoptry proteins is mutually exclusive such that parasites express one or the other, but not both.[21] Together the findings imply that microneme biogenesis occurs in multiple waves during the cell cycle with a pause during a portion of S or M/C phase for rhoptry production. In future studies, live cell imaging of fluorescent protein timers, which change color over time indicating time since synthesis, would be informative in more accurately determining when microneme and rhoptry biogenesis occurs.[52, 53]

Cell Cycle Dependence of *T. gondii* Ingestion

Endocytosis persists, but is down-regulated during the M/C phase of the cell cycle in mammalian cells.[54-56] Similar observations have been made in *Plasmodium* parasites, which undergo schizogony. This process involves a G1/trophozoite stage followed by multiple rounds of nuclear division in S phase and segmentation into many parasites in M/C phase. Endocytosis in *Plasmodium* parasites begins in G1 and is thought to remain active until the fourth nuclear division of the S phase.[30-33] However, examples of *Plasmodium* segmenters that appear to ingest red blood cell cytoplasm during the final stages of daughter cell formation have been observed.[57] We find that ingested host cytosolic proteins can be detected in *T. gondii* parasites of all cell cycle phases. Ingestion does not appear to be significantly down-regulated in any phase of the cell cycle. However, it should be noted that we were not able to enrich for M/C phase parasites. Attempts to synchronize cell cycle progression by pulse invasion as observed by Gaji *et al.* [58] were unsuccessful, because mechanically liberated parasites used to infect mCherry expressing CHO cells were not homogeneously in G0 (data not shown). This limited our power to detect a decrease in ingestion in the M/C phase.

Intersection of endocytosis and exocytosis in *T. gondii*

Ingested protein colocalizes with proM2AP and proMIC5, but not proRON4. This suggests that endocytic trafficking to the VAC intersects with exocytic trafficking to the micronemes, which contrasts with the distinct phases of endocytosis and microneme biogenesis in *Plasmodium* parasites. Microneme biogenesis begins late in the fourth nuclear division, when endocytosis is shut down.[30, 33] On the other hand, synthesis of *Plasmodium* rhoptry proteins has been observed as early as the G1/trophozoite stage.[29, 59, 60] Accordingly, endocytosis and rhoptry synthesis likely occur at the same time, opening the possibility that endocytic and exocytic trafficking also intersect in *Plasmodium.* Further, the intersection of ingested protein and microneme protein trafficking in *T. gondii* implies the existence of sorting mechanisms that ensure ingested proteins are delivered to the VAC for destruction and microneme proteins remain intact and are delivered to the microneme organelles. We speculate the existence of yet unidentified receptors for sorting of cargoes to their target organelles, discussed further below.

***T. gondii* ingestion of host cytosol does not require DrpB**

Expression of a dominant negative dynamin did not inhibit ingestion of host mCherry, suggesting that DrpB is not required for host mCherry endocytosis in *T. gondii*. However, this does not preclude the existence of DrpB-dependent endocytosis of other substrates. How host mCherry is taken up into endocytic vesicles in *T. gondii* is unclear, but could involve BAR domain proteins such as CtBP1/BARS, which have established roles in membrane fission.[61]

Interestingly, expression of ddGFP-DrpB K72A enhanced endocytosis and delivery of ingested protein to the VAC. While this could indicate the DrpB directly inhibits endocytic trafficking, this enhancement is likely indirect given the lack of interaction of the dominant negative mutant ddGFP-DrpB K72A with ingested mCherry or the endolysosomal system. ddGFP-DrpB K72A could sequester binding partners that are involved in DrpB-dependent exocytic trafficking along with liberating other partners. For example, blocking exocytic trafficking from the Golgi in mammalian cells leads to an increase in CLIC/GEEC endocytosis by freeing up the shared GTPase Arf1.[62] Dynamin hydrolyzes GTP to GDP during membrane fission and GDP is exchanged for GTP to reactivate dynamin either spontaneously or through interaction with guanine nucleotide exchange factors (GEFs).[63, 64] ddGFP-DrpB K72A is defective in GTP hydrolysis and should decrease pools of GDP-bound DrpB.[12, 48] Therefore, ddGFP-DrpB K72A expression could lead to increased rates of endocytic trafficking by increasing free pools of guanine nucleotide exchange factors required for endocytic trafficking. Alternatively, both DrpB-dependent and DrpB-independent endocytosis could exist, and shutdown of DrpB-dependent endocytosis could lead to upregulation of DrpB-independent endocytosis. Consistent with this, knockdown of core structural proteins required for endocytosis via caveolae (a dynamin-dependent endocytic pathway) leads to upregulation of the dynamin-independent CLIC-GEEC endocytic pathway.[65] Understanding the mechanisms that underlie *T. gondii* endocytosis should be a key focus going forward, especially understanding mechanisms distinguishing exocytic and

endocytic trafficking. This study provides the first glimpse into this aspect of *T. gondii* biology and suggests that DrpB is likely reserved for secretory trafficking only.

A Model for Sorting in the *T. gondii* Endolysosomal System

Taken together, we propose the following working model for intracellular trafficking in *T. gondii* (Figure 8). Because *T. gondii* replicates inside a PV, ingested proteins must traverse both the PV membrane (PVM) and the parasite plasma membrane. Studies of hemoglobin ingestion by *Plasmodium*, which also reside in a PV, showed that red blood cell cytoplasm is simultaneously taken up across the PVM and parasite plasma membrane through a mouth-like structure called the cytostome, producing double-membrane transport vesicles.[49, 57] Vesicles have been seen in the cytostome-like structure of *T. gondii* called the micropore[66], which is thought to be a site of endocytosis in the parasite, although there is no direct evidence for this. Our initial studies demonstrated that the intravacuolar network (IVN), a system of PVM-associated, membranous tubules extending into the PV lumen, is important for acquiring host proteins.[3] Using *Plasmodium* as a model, we propose that host cell cytoplasm is taken up into double-membrane transport vesicles potentially via the micropore in *T. gondii*. These transport vesicles are proposed to be the non-digestive compartment occupied at 7 min post-invasion and could be derived from endocytosis of IVN tubules or vesicles derived from the PVM. Active ingestion at 7 min post-invasion (Figure 2A) before the IVN is formed favors the existence of PVM vesicles. The IVN may contribute to ingestion indirectly through its role in organizing parasites within the PV.[67, 68] We could not conclusively determine if ingested protein colocalized with the TGN, but our data is consistent with trafficking through the ELCs. Our model represents a conservative interpretation of the data, predicting yeast or mammal-like endocytic trafficking. In this case, transport vesicles will fuse with the ELCs, releasing PVM-derived vesicles into the ELC lumen. The PVM-derived vesicles are then delivered to the VAC where they are digested. Intersection of ingested protein trafficking with exocytic trafficking to the micronemes is predicted to occur in the ELCs. How micronemes, rhoptries and ingested protein vesicles are further sorted from the ELCs to their respective target organelles is unclear and likely requires additional, unidentified sorting receptors including potential transmembrane receptors on the parasite surface that could escort PVM-derived vesicles to the VAC. Future studies will seek to better understand the molecular mechanisms of ingested protein trafficking to the VAC and sorting away from microneme proteins. Discovery of plant-like features will be particularly interesting and will provide potential targets for development of novel therapeutics that are divergent from the mammalian cells that *T. gondii* infects.

MATERIALS AND METHODS

Host Cell and Parasite Culture

All cells and parasites were maintained in a humidified incubator at 37˚C with 5% CO_2. CHO-K1 cells (ATCC® CCL-61™) were maintained in Ham's F12 supplemented with 10% FBS, 20 mM HEPES, and 2 mM L-glutamine. HFF cells (ATCC® CRL-1634™) were maintained in Dulbecco's modified Eagle's medium (DMEM) supplemented with 10% Cosmic Calf serum, 20 mM HEPES, 2 mM L-glutamine, and 50µg/ml penicillin/streptomycin. *Toxoplasma gondii* parasites were maintained by serial passaging in HFF cells. Centrin2-EGFP parasites were kindly provided by Dr. Ke Hu of Indiana University and were maintained in the presence of 1 µM pyrimethamine.[41] *RHΔhx ddFKBP-GFP-DrpB WT* and *RHΔhx ddFKBP-GFP-DrpB K72A* parasites were kindly provided by Dr. Markus Meissner of University of Glasgow. [12] *RHΔhx ddFKBP-GFP-DrpB WT* parasites had lost transgene expression in a significant portion of the population and were subcloned by limiting dilution to obtain a 100% GFP^+ population.

Generation of Parasite Lines

To generate the GalNac-YFP strain, 50µg of the pTUB GalNac YFP CAT plasmid[69] was transfected into $1.7x10^7$ RH parasites by electroporation in a 4 mm gap cuvette using a Bio-Rad Gene Pulser II set to exponential decay program with 1500 V, 25 µF capacitance and no resistance. Transfected parasites were cultured in HFF cells in the presence of chloramphenicol. Once chloramphenicol-resistant, clones were obtained by limiting dilution of the population and confirmed by immunofluorescence.

Transient Transfection of *Toxoplasma*

50µg of the pDHFR GRASP55-mRFP plasmid[69] was transfected into $1x10^8$ GalNac-YFP parasites by electroporation in a 4 mm gap cuvette in the presence of 1% DMSO using a Bio-Rad Gene Pulser II set to exponential decay with 2400 V, 25 µF capacitance and 24 Ω resistance. Transfected parasites were cultured in HFF cells for 24 to 48 h before experimentation.

Chemicals and Reagents

Morpholine urea-leucyl-homophenyl-vinylsulfone phenyl (LHVS) was kindly provided in powdered form by Dr. Matthew Bogyo at Stanford University. LHVS was dissolved in DMSO, and applied with a final DMSO concentration of 0.1-1%. Shield-1 was purchased from Clontech, resuspended in ethanol to a concentration of 1 µM and added to cultures with a final ethanol concentration of 0.08-0.1%.

Plasmids

pCMV mCherry N3 plasmid was kindly provided by Dr. Jonathan Howard Insituto Gulbenkian de Ciecia.[70] pTUB-GalNac-YFP CAT[69] and pDHFR GRASP55-mRFP[35] plasmids were kindly provided by Dr. David Roos at University of Pennsylvania. pTRE2hyg plasmid (Clontech Cat# 631014) was generously provided by Dr. Christiane Wobus at the University of Michigan.

Immunofluorescent Antibody Labeling

Purified parasites or chamberslides were fixed with 4% formaldehyde for 20 min, and washed 3 times with PBS for 5 min each. Slides were then permeabilized with 0.1% TritonX-100 for 10 min, rinsed three times in PBS, blocked with 10%FBS/0.01% Triton X-100/PBS, and incubated in primary antibodies diluted in wash buffer (1% FBS/1% NGS/0.01% Triton X-100/PBS) for 1 h at room temperature. The following primary antibodies and dilutions were used in this study. Affinity purified rabbit anti-CPL (1:100)[71], mouse anti-CPB (1:100)[72], rat anti-DrpB (1:200) kindly provided by Dr. Peter Bradley at University of California Los Angeles[12], affinity purified rabbit anti-proM2AP (1:400)[10], guinea pig anti-NHE3 kindly provided by Gustavo Arrizabalaga[36], rabbit anti-P30 (SAG1) (1:1000)[73] kindly provided by Dr. John Boothroyd at Stanford University, affinity purified mouse anti-SAG1 (US Biological) (1:1000), rabbit anti-TgPI-1 (1:500)[74] affinity purified rabbit proMIC5 (1:100)[13], mouse αRON4 mAb T5 4H1 (1:100) and mouse anti-MIC3 (1:500) kindly provided by Jean-Francois Dubremetz[42, 75], rabbit αproROP4 UVT70 (1:3000) and mouse anti-IMC1 (1:1000) kindly provided by Dr. Gary Ward of University of Vermont[20, 76], and rabbit anti-IMC1 (1:1000) kindly provided by Dr. Con Beckers of University of North Carolina, Chapel Hill.[76] Slides were washed three times and then incubated in Alex Fluor goat anti-mouse, anti-rabbit, anti-rat secondary antibody (Invitrogen Molecular Probes) diluted (1:1000) in wash buffer for 1 h at room temperature. Slides were washed three times and mounted in Mowiol before imaging.

Transfection of CHO-K1 Cells

CHO-K1 cells were plated in 35 mm dishes and transfected when they reached 70-80% confluency. Each dish was transfected with 2 µg of pCMV mCherry N3 plasmid using the X-TREMEGENE 9 Transfection Reagent (Roche, Cat# 6365787001) using a 3:1 ratio of plasmid to transfection reagent in Opti-MEM (Gibco, Cat#31985062) and a total final volume of 200 µl. Cells were then incubated overnight at 37˚C and infected at 18-24 h post-transfection.

Synchronized Invasion

Synchronous invasion was accomplished using the ENDO Buffer Method of invasion[77] with the following modifications. Briefly, parasite cultures were purified by scraping, syringing, and passing through a 3µm filter and then pelleted by spinning at 1000xg for 10 min. The pellet was then resuspended to 1-3x10^7 parasites per 1 mL in ENDO Buffer (44.7 mM K_2SO_4, 10mM $MgSO_4$, 106mM sucrose, 5 mM glucose, 20 mM Tris–H_2SO_4, 3.5 mg/ml BSA, pH 8.2) for infection of 35 mm dishes, 0.3-1x10^7 parasites per 1 mL ENDO Buffer for infection of 8-well chamber slides. Host cells were rinsed once with ENDO Buffer, and then 1 mL of ENDO Buffer-parasite suspension was added to each 35 mm dish or 100µl of ENDO Buffer-parasite suspension was added to each chamber of an 8-well chamber slide. Parasites were allowed to settle at 37˚C for 10 min before the ENDO Buffer was removed and replaced with twice the volume of Invasion Media (Ham's F12/3% Cosmic Calf Serum/20 µM HEPES). Parasites were allowed to invade at 37˚C for 7 or 10 min as indicated. Cells were washed three times with warm media to remove uninvaded parasites and placed back at 37˚C until ready for purification or fixation.

Protease Protection Assay

Protease protection assay was performed as described previously.[3] Briefly, purified parasites were pelleted for 10 min at 1000xg at 4˚C, supernatant was removed, and resuspended in 250 µl of freshly prepared 1 mg/mL Pronase (Roche, Cat# 10165921001)/0.01% Saponin/PBS and incubated at 12˚C for 1 h. Reaction was stopped with the addition of 5 mL ice cold PBS.

Intracellular Fluorescent Protein Acquisition Assay

Transfected CHO-K1 cells were synchronously invaded by the ENDO Buffer method with *T. gondii* parasites, treated with LHVS or equal volume of DMSO for the indicated time prior to harvest, and purified at the indicated times post-invasion as previously described.[3] For ddGFP-DrpB strains, EtOH or Shield-1 were also added for the indicated amounts of time prior to harvest to induce DrpB WT or K72A expression. All subsequent harvesting steps are performed on ice or at 4˚C unless otherwise noted. Infected cells were washed twice with ice-cold PBS to remove any extracellular parasites, and intracellular parasites were liberated and purified by scraping and syringing with a 5/8" 25g needle before passing through a 3 µm filter. Parasites were then subjected to the protease protection assay, pelleted by spinning at 1000xg for 10 min and washed three times in ice cold PBS before depositing on Cell-Tak (Corning, Cat# 354240) coated chamber slides. Parasites were fixed and stained with the indicated antibodies.

Assessment of ingestion and localization

Imaging was performed at 63x with an AxioCAM MRm camera-equipped Zeiss Axiovert Observer Z1 inverted fluorescence microscope. Ingestion of host mCherry was scored manually as mCherry positive or mCherry negative. Colocalization of ingested mCherry and endolysosomal markers was scored manually with each individual puncta of ingested mCherry or endolysosomal marker signal being scored using a binary measure of colocalized or not. This gives a readout of percent puncta colocalized with a given endolysosomal marker within each experiment. Ingested mCherry or endolysosomal marker puncta were scored as colocalized if they showed any overlap, and there was no differentiation between complete or partial colocalization. An independent, blinded observer validated the colocalization findings for ingested mCherry by reanalyzing 15 percent of the colocalization data. Their findings confirmed the reported results.

Detection of MIC3 Secretion into the PV

HFF chamber slides were synchronously invaded with ddFKBP-GFP-DrpB WT or K72A parasites by the ENDO Buffer Method and treated with ethanol or Sh-1 for the indicated amounts of

time immediately prior to fixation at 6 h post-invasion. Chamber slides were fixed and stained for MIC3 and TgPI-1 as described above, except cells were partially permeablized with 0.02% w/v saponin for staining of the PV lumen but not the parasite interior. Cells were then blocked with 10%FBS/PBS, and incubated in primary and secondary antibodies diluted in wash buffer without detergent (1% FBS/1% NGS/PBS) to stain MIC3 as a representative microneme protein and the dense granule protein TgPI-1 as a control stain for the PV lumen. %MIC3$^+$ vacuoles were determined by scoring of TgPI-1$^+$ vacuoles for MIC3 staining.

Generating CHO-K1 inducible mCherry Cells

A plasmid expressing mCherry under a tetracycline-inducible minimal CMV promoter was generated by inserting mCherry into the pTRE2hyg plasmid (Clontech Cat# 631014) using Gibson Assembly. mCherry was amplified from the pmCherry N3 plasmid using the forward primer 5'-ctagtcagctgacgcgtgatggtgagca agggcgag-3' and reverse primer 5'-tcgatgcggccgcgctagttacttgtacagctcgtc-3'. The pTRE2 plasmid was cut within the multiple cloning site using NheI, and mCherry was inserted by homologous recombination using Gibson Assembly Master Mix (NEB, Cat# E2611S) to generate the plasmid pTRE2-mCherry. Insertion was confirmed by sequencing. pTRE2-mCherry and pTet-On (Clontech, Cat# 631018), expressing the reverse tet-responsive transcriptional activator, were cotransfected into CHO-K1 cells and selected with 200 µg/mL hygromycin B (Invitrogen, Cat# 10687010) and 400 µg/mL geneticin (Invitrogen, Cat# 10131035). After recovery from drug selection, the cells were maintained in culture with 200µg/mL hygromycin B and 400 µg/mL geneticin, sorted for the brightest mCherry signal following treatment with doxycycline (Clontech, Cat# 63111) by live fluorescence-associated cell sorting and cloned out. Clones were chosen based on screening for lack of signal in the absence of doxycycline and intensity of mCherry following treatment with addition of 1 µg/mL doxycycline for 48 h. Fluorescence intensity as compared to transiently transfected CHO-K1 WT cells was evaluated using flow cytometry using a BD LSRFortessa Cell Analyzer with FACSDiva software.

Green-blue invasion assay for viability of mCherry$^+$ parasites

Ability of mCherry$^+$ parasites to invade host cells was determined using a modified red-green invasion assay.[78] The ntracellular fluorescent protein acquisition assay was performed with RH parasites treated with 1µM LHVS for 36 h harvested from iCHO imCh cells at 3 hpi with the following modifications. Protease protection assay was not performed, and instead, parasites were resuspended in 100 µl DMEM/10% Cosmic Calf serum/20 mM HEPES/2 mM L-glutamine/50µg/ml penicillin/streptomycin/1µM LHVS and allowed to invade HFF cells in an 8-chamber slide for 30 min at 37°C. Treatment with 1 µM LHVS during the invasion period was performed to prevent mCherry degradation. The chamber slide was then gently washed to remove uninvaded and unattached parasites, fixed with 4% formaldehyde for 20 min, and washed 3 times with PBS for 5 min each. Extracellular parasites were stained by blocking with 10%FBS/PBS followed by incubation with rabbit anti-SAG-1 diluted in wash buffer without detergent (1% FBS/1% NGS/PBS) for 1 h at room temperature. Both intracellular and extracellular parasites were then stained with mouse anti-SAG-1 or mouse anti-CPL according to the immunofluorescent antibody labeling protocol above beginning with Triton X-100 permeablization.

ACKNOWLEDGMENTS

We gratefully acknowledge funding to support this work including NIH T32 Molecular Mechanisms of Microbial Pathogenesis (5T32AI007528 to O.L.M), NIH Ruth L. Kirschstein F31- Diversity (1F31AI118274-01 to O.L.M), and ASM Robert D. Watkins Graduate Research Fellowship (to O.L.M.) and an NIH operating grant (R01AI120607 to V.B.C.). We thank our colleagues Jonathan Howard, Markus Meissner, Christiane Wobus, John Boothroyd, Peter Bradley, Gustavo Arrizabalaga, Jean-Francois Dubremetz, Gary Ward, and Con Beckers for providing key reagents. We also thank Sophina Taitano for providing assistance and expertise in flow cytometry and My-Hang Huynh for critically reading this manuscript before submission. There are no conflicts of interest to report.

FIGURE LEGENDS

FIGURE 1 Ingested host cytosolic mCherry is associated with the ELCs, VAC, and possibly the TGN. A, Experimental design for detection and localization of host cytosolic protein ingestion. CHO-K1 cells were transiently transfected with a plasmid encoding cytosolic mCherry fluorescent protein 18-24 h before synchronous invasion for 10 min with *T. gondii* parasites (pretreated with 1µM LHVS or the vehicle control DMSO for 36 h). Parasites were allowed to ingest host cytosol for 3 h in the presence of 1 µM LHVS or DMSO before being purified, stained and analyzed by fluorescence microscopy. B-D, Quantitation of ingestion of host cytosolic mCherry in WT, GalNac-YFP or ddGFP-DrpB WT parasites treated with 1 µM LHVS or DMSO. ddGFP-DrpB WT parasites were also treated with ethanol (EtOH) or 0.8µM Sh-1 for 30 min beginning at 2.5 h post-invasion to induce expression of DrpB WT. Shown is

percentage of mCherry positive parasites, at least 200 parasites analyzed per condition, ratio paired t-test for B and C, one-way ANOVA with Tukey's multiple comparisons for D. E, Representative images for localization of ingested mCherry in LHVS-treated parasites from B-D relative to the apicoplast using DAPI staining, CPB, NHE3 or proM2AP using antibody staining, GalNac-YFP or GFP-DrpB WT. Scale bars: 2μm. Blue arrowhead indicates the apicoplast, and white arrows indicate areas of colocalization when the endolysosomal marker of interest has several puncta. F, Quantitation of colocalization of ingested mCherry with the indicated markers of the endolysosomal system. At least 30 ingested mCherry puncta per marker, one-way ANOVA with Dunnet's test for multiple comparisons to colocalization with the apicoplast. Only significant associations shown, Apicoplast vs. NHE3 is not significant. All bars represent mean from 3 or more biological replicates with standard deviation error bars. * $p<0.05$, ** p,<0.01, ***$p<0.001$, ****$p<0.0001$, ns is not significant.

FIGURE 2 Host cytosolic mCherry is ingested into a non-digestive compartment before delivery to the VAC within 30 min. A, Time course of ingestion in DMSO or LHVS-treated GalNac-YFP parasites through 1 h post-invasion. Experiment performed as in Figure 1A, but with a 7 min invasion period and harvested at the indicated times. Shown is percentage of mCherry positive parasites from analysis of at least 200 parasites analyzed per condition and time point. Ratio paired t-test comparing DMSO vs. LHVS treatment at each time point, * $p<0.05$, otherwise not significant. B, Quantitation of colocalization of ingested mCherry with CPB/L in LHVS-treated parasites from A stained with mouse antibodies against both CPB and CPL. At least 30 ingested mCherry puncta were analyzed per marker and time point. C, Representative images for localization of ingested mCherry relative CPB/L. Scale bars, 2 μm: For all graphs, points represent the mean of 3 biological replicates, bars represent standard deviation.

FIGURE 3 Microneme proteins are expressed in G, S and M/C phase. A and B, Representative images for detection of proM2AP or proMIC5 by immunofluorescent staining in G, S and M/C phase Cen2-EGFP vacuoles stained for IMC1 at 4 to 6 h post-invasion. C and D, Quantitation of percentage of Cen2-EGFP vacuoles positive for proM2AP or proMIC5 staining in G, S and M/C phase at 4 to 6 h post-invasion. E and F, Representative images for detection of proM2AP or proMIC5 by immunofluorescent staining in G, S and M/C phase Cen2-EGFP vacuoles stained for IMC1 at 24 h post-invasion. G and H, Quantitation of percentage of Cen2-EGFP vacuoles positive for proM2AP or proMIC5 staining in G, S and M/C phase at 24 h post-invasion. Error bars in all graphs represent standard deviation, and the point where the grey fill intersects the error bars represents the mean. Values derived from 3 biological replicates each with at least 100 total vacuoles and at least 30 vacuoles per cell cycle phase analyzed. Scale bars: 2 μm.

FIGURE 4 Rhoptry proteins are expressed in S and M/C phase. A, Representative images for detection of proROP4 by immunofluorescent staining in G, S and M/C phase Cen2-EGFP vacuoles at 4 to 6 h post-invasion. B, Quantitation of percentage of Cen2-EGFP vacuoles positive for proROP4 staining in G, S and M/C phase at 4 to 6 h post-invasion. C and D, Representative images for detection of proROP4 or proRON4 by immunofluorescent staining in G, S and M/C phase Cen2-EGFP vacuoles at 24 h post-invasion. E and F, Quantitation of percentage of Cen2-EGFP vacuoles positive for proROP4 or proRON4 staining in G, S and M/C phase at 24 h post-invasion. Error bars in all graphs represent standard deviation, and the point where the grey fill intersects the error bars represents the mean. Values are derived from 3 biological replicates each with at least 100 total vacuoles and at least 30 vacuoles per cell cycle phase analyzed. Scale bars: 2 μm.

FIGURE 5 *T. gondii* ingests host cytosolic mCherry throughout its cell cycle. A, Experimental design for detection and localization of recently ingested host cytosolic protein ingestion. CHO-K1 cells were transiently transfected with a plasmid encoding cytosolic mCherry fluorescent protein 18-24 h before synchronous invasion for 10 min with untreated *T. gondii* parasites. 50 μM LHVS or DMSO added during the last 30 min of infection before being purified, stained and analyzed by fluorescence microscopy. B, Quantitation of ingestion in Cen2-EGFP parasites treated with DMSO or LHVS for 36 h or 30 min and purified at 3 h post-invasion. Shown is percentage of mCherry positive parasites, at least 200 parasites analyzed per condition, One-way ANOVA with Tukey's multiple comparisons. C, Cell cycle phasing of LHVS-treated Cen2-EGFP parasites harvested at 4 to 6 h post-invasion to be quantitated for ingestion in D as determined by pattern of Cen2-EGFP and antibody staining for IMC1. D, Quantitation of ingestion in DMSO or LHVS-treated Cen2-EGFP parasites at 4 to 6 h post-invasion. Shown is percentage of mCherry positive parasites, at least 200 parasites analyzed per condition, ratio paired t-test. E, Representative images for detection of ingested host cytosolic mCherry in parasites in G, S or M/C phase. F, Cell cycle phase-specific analysis of ingestion pathway activity. Percentage of mCherry positive parasites in each cell cycle phase from parasites in D was determined with at least 230 parasites in G phase, at least 55 parasites in S phase and at least 24 parasites in M/C phase analyzed, one way ANOVA. All bars represent the mean of 4 biological replicates, error bars represent standard deviation, ** $p<0.01$, ns = not significant, scale bars are 2 μm.

FIGURE 6 Endocytic trafficking is merged with microneme biogenesis in *T. gondii*. A, Quantitation of mCherry ingestion in DMSO or LHVS-treated WT parasites at 3 h post-invasion. Experiment carried out as in Figure S5 with infection of CHO-K1 imCh cells and 200

μM LHVS treatment for 30 min to detect recently ingested mCherry only. Shown is percentage of mCherry positive parasites, at least 200 parasites analyzed per condition, unpaired t-test. B, Quantitation of ingestion pathway activity during microneme biogenesis by comparing proMIC5 positive and negative populations. Shown is percentage of mCherry positive parasites, at least 200 parasites analyzed for each proMIC5 positive and negative population, ratio paired t-test. C, Quantitation of ingestion pathway activity during rhoptry biogenesis by comparing proRON4 positive and negative populations. Shown is percentage of mCherry positive parasites, at least 200 parasites for each proRON4 positive and negative population, ratio paired t-test. D, Quantitation of colocalization of ingested mCherry with proM2AP, proMIC5, proRON4 or the apicoplast in LHVS-treated parasites from A stained with antibodies each indicated marker. At least 30 ingested mCherry puncta analyzed per marker. One-way ANOVA with Dunnet's test for multiple comparisons to colocalization with the apicoplast. E, Representative images of localization of ingested mCherry relative to proM2AP, proMIC5, proRON4 or the apicoplast (indicated by the blue arrow head). All bars represent the mean from 3 biological replicates, error bars represent standard deviation, ** p,<0.01, ***p<0.001, ns = not significant, scale bars are 2 μm.

FIGURE 7 Ingestion does not require DrpB. A, Representative images for aberrant secretion of MIC3 into the PV lumen in ddGFP-DrpB K72A parasites with the addition of Shield-1 (Sh-1), but not the vehicle control ethanol (EtOH). Synchronously-infected cells were treated with 1 μM Sh-1 or the vehicle control ethanol (EtOH) for 5 h, partially permeablized with 0.02% saponin to allow staining of the PV lumen, but not the parasite interior, and stained with antibodies against MIC3 and against the dense granule protein TgPI-1 as a positive control for PV lumen staining. Scale bars: 2 μm. B, Quantitation of aberrant MIC3 secretion into the PV lumen in ddGFP-DrpB K72A parasites treated as in A with 1μM Shield-1 (Sh-1) for the last 2, 3 or 5 h of infection or 5 h for ethanol (EtOH). Shown is percentage of TgPI-1^{+} vacuoles that are MIC3^{+}, at least 100 vacuoles scored in each of 3 biological replicates. One-way ANOVA with Dunnet's test for multiple comparisons to the EtOH control. C and D, Quantitation of mCherry ingestion in ddGFP-DrpB K72A and RH parasites. Conducted as in Figure S5A, treated with 0.2% DMSO or 200 μM LHVS for 30 min and 0.1% EtOH or 1μM Sh-1 for the indicated amounts of time in C and 3 h in D. Shown is percentage of mCherry positive parasites, with at least 200 parasites analyzed for each of 2 biological replicates for DMSO+Shield-1 in C, and at least 3 biological replicates for all other samples. One-way ANOVA with Dunnet's test for multiple comparisons of LHVS+EtOH treated samples to the DMSO+EtOH treated control are not shown, but all comparisons are significant. Unpaired, two-sample t-tests for comparison of EtOH and Sh-1 treated samples shown. E, Quantitation of colocalization of ingested mCherry with GFP-DrpB K72A, proM2AP and CPL by antibody staining, or the apicoplast by DAPI staining in LHVS-treated ddGFP-DrpB K72A parasites from D. At least 30 ingested mCherry puncta were analyzed per marker for each of 4 biological replicates for CPL and 3 biological replicates for all other markers. One-way ANOVA with Dunnet's test for multiple comparisons of EtOH treated samples to the apicoplast are not shown, but proM2AP and CPL comparisons are significant. Unpaired two-sample t-tests for comparison of EtOH and Sh-1 treated samples for each marker and comparison of the apicoplast and ddGFP-DrpB K72A in Sh-1 treated parasites shown. F, Quantitation of colocalization of CPL with the indicated markers by antibody staining in intracellular ddGFP-DrpB K72A parasites synchronously invaded into HFF cells, treated with 0.1% EtOH or 1μM Sh-1 for 3 h and fixed at 3 h post-invasion. At least 40 CPL puncta analyzed per marker for each of 3 biological replicates. Unpaired two-sample t-tests for comparison of EtOH and Sh-1 treated samples. G and H, Representative images for colocalization of ddGFP-DrpB WT or ddGFP-DrpB K72A with the indicated markers by antibody staining, quantitated in I. White arrows indicate regions of colocalization. Scale bars: 5 μm. I, Quantitation of colocalization of Sh-1 treated ddGFP-DrpB WT or ddGFP-DrpB K72A with the indicated endolysosomal markers by antibody staining or the apicoplast by DAPI staining in intracellular parasites treated as in F with ddGFP-DrpB WT parasites treated with 0.8 μM Sh-1 for 30 min and ddGFP-DrpB K72A parasites treated with 1.0 μM Sh-1 for 3 h. At least 40 DrpB puncta analyzed per marker, per replicate for 3 biological replicates. One-way ANOVA with Dunnet's test for multiple comparisons of each marker to the apicoplast for each ddGFP-DrpB WT and ddGFP-DrpB K72A parasites, only significant results shown. Unpaired two-sample t-tests for comparison of localization in ddGFP-DrpB WT vs. K72A. All bars represent means and error bars represent standard deviation. *p<0.05, **p<0.01, ***p<0.001, ns is not significant.

FIGURE 8 Working model for trafficking and sorting of endocytic and exocytic cargoes in *T. gondii.* 1. Host cell cytosol (red) is taken up across the PVM and parasite plasma membrane into double membrane transport vesicles, potentially at the micropore. 2. These transport vesicles then fuse with the ELCs and deliver the host cytosol-containing, PVM-derived vesicles to the ELC lumen, where we propose ingested protein trafficking intersects with trafficking of microneme proteins. 3. Fusion of the ELCs with the VAC would then deliver the PVM-derived vesicles to the lumen of the VAC. How the PVM-derived vesicles are sorted away from the microneme proteins is unclear. Trafficking to the VAC may represent a bulk flow pathway independent of receptor-mediated uptake and sorting, or it could require unidentified receptors that recognize parasite proteins associated with the PVM-derived vesicles. This model depicts the possibility of receptor-mediated uptake of PVM-derived vesicles at the parasite plasma membrane and escorting them all the way to the VAC. 4. In the VAC, the PVM-derived vesicles are presumably ruptured by parasite lipases, releasing host cytosolic proteins and exposing them to degradation by parasite proteases. 5. Immature microneme and rhoptry proteins are escorted to the ELCs by TgSORTLR where their propeptides are cleaved off by proteases. However, trafficking at some point diverges so that trafficking of

microneme proteins intersect with ingested protein, but rhoptry proteins do not and may occupy a distinct subset of ELCs. 6. Microneme and rhoptry proteins are sorted from the ELCs to their respective organelles by unknown mechanisms that likely involve unidentified receptors.

SUPPLEMENTARY FIGURE LEGENDS

FIGURE S1 Localization of GalNac-YFP in RH GalNac-YFP parasites and viability of mCherry+ parasites. Representative images for localization of GalNac-YFP in RH GalNac-YFP parasites. GalNac-YFP parasites or GalNac-YFP parasites transiently transfected to express GRASP55-RFP were synchronously infected in HFF cells, fixed at 3 h post-invasion and stained with DAPI to label the apicoplast or CPB, CPL, NHE3, proM2AP and/or DrpB using antibody staining. Blue arrowhead indicates the apicoplast, and white arrows indicate "Golgi-free" GalNac-YFP signal. Images are representative of two biological replicates. Scale bars: 2 μm, ns is not significant.

FIGURE S2 Localization and secretory function of ddGFP-DrpB WT. A, Representative images for lack of aberrant secretion of MIC3 into the PV lumen in ddGFP-DrpB WT and ddGFP-DrpB K72A dominant negative mutant parasites, which have a known defect in MIC3 trafficking resulting in secretion into the PV lumen. Synchronously-infected cells were treated with 1 μM Sh-1 or the vehicle control ethanol (EtOH) for 6h, partially permeablized with 0.02% saponin to allow staining of the PV lumen but not the parasite interior and stained with antibodies against MIC3 and against the dense granule protein TgPI-1 as a positive control for PV lumen staining. B, Quantitation of aberrant MIC3 secretion into the PV lumen in ddGFP-DrpB WT parasites treated with 1μM Sh-1 for the last 0.5, 1 or 6 h of infection or 6h with EtOH and fixed at 6 h post-invasion or ddGFP-DrpB K72A parasites treated with 1 μM Sh-1 for 6h as a positive control. Shown is percentage of TgPI-1^{+} vacuoles that are MIC3^{+}, at least 100 vacuoles scored in each of two biological replicates. One-way ANOVA with Dunnet's test for multiple comparisons to the EtOH control, only significant results shown. C, Representative images for localization of DrpB in RHΔhx ddFKBP-GFP-DrpB WT (top panels) and RH parasites (bottom panels). Parasites were synchronously invaded into HFF cells and fixed at 3 h post-invasion. ddGFP-DrpB WT parasites were treated with 0.8 μM Sh-1 for the last 30 min of infection, RH parasites were stained with DrpB antibodies, and both parasite strains were stained with DAPI to label the apicoplast or antibodies to label CPL, NHE3 or proM2AP. Blue arrowheads indicate the apicoplast. Images are representative of two biological replicates for RH and three biological replicates for ddGFP-DrpB parasites. All scale bars: 2 μm, bars represent means, error bars represent standard deviation, *p<0.05.

FIGURE S3 mCherry^{+} parasites are viable and ingested mCherry colocalizes with GalNac-YFP in a CPB positive compartment. A, Harvested mCherry^{+} parasites are viable and can invade HFF cells. Representative images for mCherry associated with extracellular (EC) and intracellular (IC) parasites. Ingestion assay performed with RH parasites as described in Figure 1A using CHO imCherry cells (described in Figure S5) to maximize mCherry^{+} parasites (see Figure S5C). Following harvest, parasites were resuspended in DMEM/10% cosmic calf serum/20 mM HEPES/2 mM L-glutamine/50μg/ml penicillin/streptomycin treated with 1μM LHVS to inhibit ingested mCherry turnover during the invasion period, and a green-blue invasion assay was performed. Rabbit anti-SAG1 (blue) indicates EC parasites and mouse anti-SAG1 (green) will label all parasites. Images are representative of two biological replicates. B, Quantitation of ingestion in EC versus IC parasites depicted in A. Shown is percentage of mCherry positive parasites, at least 100 parasites analyzed for each of two biological replicates, unpaired two-sample t-test. C, Representative images for mCherry in IC parasites colocalizing with CPL. Parasites treated as in A, but stained with mouse anti-CPL instead of mouse anti-SAG1. CPL colocalized with 77.6% (13/17) ingested mCherry puncta, suggesting the mCherry is contained within the parasites. One biological replicate. D, Representative images for localization of ingested mCherry relative to GalNac-YFP and CPB in LHVS-treated GalNac-YFP parasites stained for CPB from Figure 1. From top to bottom are examples of ingested mCherry colocalized with GalNac-YFP only, CPB only, both GalNac-YFP and CPB, and neither GalNac-YFP or CPB. White arrows indicate localization of ingested mCherry accumulation. E, Quantitation of colocalization of ingested mCherry with GalNac-YFP and/or CPB in LHVS-treated GalNac-YFP parasites stained for CPB from Figure 1. Data are derived from 4 biological replicates with at least 30 ingested mCherry puncta analyzed per marker, per replicate. F, Quantitation of colocalization of GalNac-YFP with CPB and CPL in intracellular DMSO and LHVS-treated parasites. HFF cells were synchronously invaded with GalNac-YFP parasites treated with DMSO or LHVS as in Figure 1, and fixed at 3 h post-invasion. Parasites were then stained with antibodies against CPB and CPL and analyzed by fluorescence microscopy. Data are derived from 2 biological replicates with at least 33 GalNac-YFP puncta analyzed per replicate. G, Representative images of GalNac-YFP distribution with DMSO or LHVS treatment as in C and stained for NHE3 and CPB. Scale bars, 1μM. H, Quantitation of colocalization of the GalNac-YFP^{+}CPB^{+} compartment with other endolysosomal system markers. GalNac-YFP parasites were treated as in C and stained for CPB and CPL, proM2AP, NHE3, or DAPI to label the apicoplast. Data are derived from 3 biological replicates with at leasActiveUt 20 GalNac-YFP^{+}CPB^{+} puncta analyzed per marker, per replicate, one way ANOVA with Dunnet's test for

multiple comparisons to colocalization with the apicoplast, ** p,<0.01, ***p<0.001. All bars represent means, and error bars represent standard deviation. Scale bars: 2μm unless otherwise noted.

FIGURE S4 *T. gondii* ingests host cytosolic mCherry within 7 min post-invasion, and peak colocalization with the GalNac-YFP^{+}CPB/L^{+} compartment coincides with rapid degradation of ingested material. A, mCherry accumulation is contained within the SAG1 surface outline of the parasites at 7 min post-invasion. Experiment performed as in Figure 2, parasites were purified immediately following invasion (7 min post-invasion), and stained for the parasite surface marker SAG1. No protease protection assay was performed (No Pronase), leaving SAG1 on the surface of the parasite. Shown are cut views from Z-stacks displaying a single plane that cuts through the center of the accumulated mCherry signal. B, mCherry accumulation, but not SAG1 is resistant to protease protection assay (Pronase). Experiment performed as in A but were subjected to protease protection assay, and stained for the parasite surface marker SAG1. In parasites where SAG1 was digested off the parasite surface, mCherry accumulation remains. One biological replicate for A and B, performed in GalNac-YFP parasites treated with DMSO or 1μM LHVS for 36 h or *RH*Δ*cpl* parasites as indicated. Scale bars: 2μm. C, Quantitation of colocalization of ingested mCherry with GalNac YFP or CPB/L in LHVS-treated parasites from Figure 2. At least 30 ingested mCherry puncta analyzed per marker and time point. Points represent the mean of 3 biological replicates, bars represent standard deviation.

FIGURE S5 Validation of CHO-K1 imCherry cell line for detection of ingestion. A, Conceptual model for mCherry expression in CHO-K1 inducible mCherry (CHO-K1 imCh) cell. CHO-K1 cells that stably express mCherry under the control of the minimal CMV promoter and the tetracycline-responsive element (TRE) as well as the reverse tetracycline-controlled transactivator (rtTA) were generated. In the absence of tetracycline or its derivative doxycycline, rtTA cannot bind the TRE, and cytosolic mCherry transcription is repressed. In the presence of doxycycline, doxycycline will bind to rtTA and allow it to bind to the TRE and induce transcription of cytosolic mCherry. B, From top to bottom, representative images of mCherry detection in the parental CHO-K1 WT cell line, CHO-K1 WT cells transiently transfected with the pmCherry N3 plasmid, CHO-K1 imCh cells without DOX for 96 h and CHO-K1 imCh cells treated with 2μg/mL DOX for 96 h. To the right are values for the percentage of cells that are mCherry positive (%mCh^{+}) and mean fluorescence intensity of the mCherry (MFI) as determined by flow cytometry. Data derived from 2 biological replicates with 20,000 cells analyzed per condition per replicate. Scale bar, 20μm. C, Quantitation of ingestion of host cytosolic mCherry from CHO-K1 WT, CHO-K1 WT cells transiently transfected to express cytosolic mCherry, CHO-K1 imCh cells without DOX for 96 h and CHO K1-imCh cells with 2μg/mL DOX for 96 h. Cells were synchronously invaded for 10 min with WT parasites treated with DMSO or LHVS as indicated, purified at 3 h post-invasion, fixed and analyzed by fluorescence microscopy. Shown is percentage of mCherry positive parasites with at least 200 parasites analyzed per condition, one way ANOVA with Tukey's test for multiple comparisons, ** p<0.01, ***p<0.001, ns = not significant. D, Representative images of detection of ingested mCherry from parasites in C. Scale bars: 5μm.

REFERENCES

1. Montoya J, Giraldo L, Efron B, et al. Infectious complications among 620 consecutive heart transplant patients at Stanford University Medical Center. *Clin Infect Dis*. 2001;33:629-640.
2. Hoffmann S, Batz MB, Morris JG,Jr. Annual cost of illness and quality-adjusted life year losses in the United States due to 14 foodborne pathogens. *J Food Prot*. 2012;75(7):1292-1302. doi: 10.4315/0362-028X.JFP-11-417.
3. Dou Z, McGovern O, Di Cristina M, Carruthers V. *Toxoplasma gondii* ingests and digests host cytosolic proteins. . *mBio*. 2014;5(4):e01188-14.
4. Di Cristina M, Dou Z, Lunghi M, et al. *Toxoplasma* depends on lysosomal consumption of autophagosomes for persistent infection. *Nat Microbiol*. 2017;2:17096. doi: 10.1038/nmicrobiol.2017.96.
5. Stenmark H. Rab GTPases as coordinators of vesicle traffic. *Nat Rev Mol Cell Biol*. 2009;10(8):513-525. doi: 10.1038/nrm2728.
6. Dettmer J, Hong-Hermesdorf A, Stierhof Y, Schumacher K. Vacuolar H+-ATPase activity is required for endocytic and secretory trafficking in *Arabidopsis*. *Plant Cell*. 2006;18:715-730.
7. Tomavo S, Slomianny C, Meissner M, Carruthers VB. Protein trafficking through the endosomal system prepares intracellular parasites for a home invasion. *PLoS Pathog*. 2013;9(10):e1003629. doi: 10.1371/journal.ppat.1003629.

8. Miranda K, Pace DA, Cintron R, et al. Characterization of a novel organelle in *Toxoplasma gondii* with similar composition and function to the plant vacuole. *Mol Microbiol*. 2010;76(6):1358-1375. doi: 10.1111/j.1365-2958.2010.07165.x.
9. Pieperhoff MS, Schmitt M, Ferguson DJ, Meissner M. The role of clathrin in post-Golgi trafficking in *Toxoplasma gondii. PLoS One*. 2013;8(10):e77620. doi: 10.1371/journal.pone.0077620
10. Harper JM, Huynh MH, Coppens I, Parussini F, Moreno S, Carruthers VB. A cleavable propeptide influences *Toxoplasma* infection by facilitating the trafficking and secretion of the TgMIC2-M2AP invasion complex. *Mol Biol Cell*. 2006;17(10):4551-4563. doi: E06-01-0064 [pii]; 10.1091/mbc.E06-01-0064.
11. Kremer K, Kamin D, Rittweger E, et al. An Overexpression Screen of *Toxoplasma gondii* Rab-GTPases Reveals Distinct Transport Routes to the Micronemes. *PLoS Pathog*. 2013;9(3):e1003213. doi: 10.1371/journal.ppat.1003213; 10.1371/journal.ppat.1003213.
12. Breinich MS, Ferguson DJ, Foth BJ, et al. A dynamin is required for the biogenesis of secretory organelles in *Toxoplasma gondii. Curr Biol*. 2009;19(4):277-286. doi: 10.1016/j.cub.2009.01.039.
13. Brydges SD, Harper JM, Parussini F, Coppens I, Carruthers VB. A transient forward-targeting element for microneme-regulated secretion in *Toxoplasma gondii. Biol Cell*. 2008;100(4):253-264. doi: 10.1042/BC20070076.
14. Sangare LO, Alayi TD, Westermann B, et al. Unconventional endosome-like compartment and retromer complex in *Toxoplasma gondii* govern parasite integrity and host infection. *Nat Commun*. 2016;7:11191. doi: 10.1038/ncomms11191.
15. Sloves PJ, Delhaye S, Mouveaux T, et al. *Toxoplasma* sortilin-like receptor regulates protein transport and is essential for apical secretory organelle biogenesis and host infection. *Cell Host Microbe*. 2012;11(5):515-527. doi: 10.1016/j.chom.2012.03.006; 10.1016/j.chom.2012.03.006.
16. Venugopal K, Werkmeister E, Barois N, et al. Dual role of the *Toxoplasma gondii* clathrin adaptor AP1 in the sorting of rhoptry and microneme proteins and in parasite division. *PLoS Pathog*. 2017 Apr 21;13(4):e1006331.
17. Bargieri D, Lagal V, Andenmatten N, Tardieux I, Meissner M, Ménard R. Host Cell Invasion by Apicomplexan Parasites: The Junction Conundrum. *PLoS Pathog*. 2014 Sep 18;10(9):e1004273. doi: 10.1371/journal.ppat.1004273. eCollection 2014 Sep.
18. Dowse T, Soldati D. Host cell invasion by the apicomplexans: the significance of microneme protein proteolysis. *Curr Opin Microbiol*. 2004;7(4):388-396. doi: 10.1016/j.mib.2004.06.013.
19. Hunter CA, Sibley LD. Modulation of innate immunity by *Toxoplasma gondii* virulence effectors. *Nat Rev Microbiol*. 2012;10(11):766-778. doi: 10.1038/nrmicro2858; 10.1038/nrmicro2858.
20. Carey KL, Jongco AM, Kim K, Ward GE. *The Toxoplasma go*ndii rhoptry protein ROP4 is secreted into the parasitophorous vacuole and becomes phosphorylated in infected cells. *Eukaryot Cell*. 2004;3(5):1320-30.
21. Besteiro S, Michelin A, Poncet J, Dubremetz J, Lebrun M. Export of a *Toxoplasma gondii* Rhoptry Neck Protein Complex at the Host Cell Membrane to Form the Moving Junction during Invasion. *PLoS Pathog*. 2009;Feb;5(2):e1000309.
22. Etheridge RD, Alaganan A, Tang K, Lou HJ, Turk BE, Sibley LD. The *Toxoplasma* pseudokinase ROP5 forms complexes with ROP18 and ROP17 kinases that synergize to control acute virulence in mice. *Cell Host Microbe*. 2014 May 14;15(5):537-550.
23. Huynh MH, Carruthers VB. A *Toxoplasma gondii* Ortholog of Plasmodium GAMA Contributes to Parasite Attachment and Cell Invasion. *mSphere*. 2016;1(1):10.1128/mSphere.00012-16. eCollection 2016 Jan-Feb. doi: 10.1128/mSphere.00012-16.
24. Huynh MH, Boulanger MJ, Carruthers VB. A conserved apicomplexan microneme protein contributes to *T. gondii* invasion and virulence. *Infect Immun*. 2014. doi: IAI.01877-14 [pii].
25. Sidik SM, Huet D, Ganesan SM, et al. A Genome-wide CRISPR Screen in *Toxoplasma* Identifies Essential Apicomplexan Genes. *Cell*. 2016;166(6):1423-1435.e12. doi: 10.1016/j.cell.2016.08.019.
26. Kafsack BF, Pena JD, Coppens I, Ravindran S, Boothroyd JC, Carruthers VB. Rapid membrane disruption by a perforin-like protein facilitates parasite exit from host cells. *Science*. 2009;323(5913):530-533. doi: 10.1126/science.1165740.
27. Guérin A, Corrales RM, Parker ML, et al. Efficient invasion by *Toxoplasma* depends on the subversion of host protein networks. *Nat Microbiol*. 2017 Aug 28;doi: 10.1038/s41564-017-0018-1.
28. Futter CE, Connolly CN, Cutler DF, Hopkins CR. Newly synthesized transferrin receptors can be detected in the endosome before they appear on the cell surface. *J Biol Chem*. 1995 May 5;270(18):10999-11003.
29. Margos G, Bannister LH, Dluzewski AR, Hopkins J, Williams IT, Mitchell GH. Correlation of structural development and differential expression of invasion-related molecules in schizonts of *Plasmodium falciparum*. *Parasitology*. 2004 Sep;129(Pt 3):273-287.
30. Hanssen E, Knoechel C, Dearnley M, et al. Soft X-ray microscopy analysis of cell volume and hemoglobin content in erythrocytes infected with asexual and sexual stages of Plasmodium falciparum. *J Struct Biol*. 2012;177(2):224-232. doi: 10.1016/j.jsb.2011.09.003.
31. Francis SE, Gluzman IY, Oksman A, et al. Molecular characterization and inhibition of a *Plasmodium falciparum* aspartic hemoglobinase. *EMBO J*. 1994 Jan 15;13(2):306-317.

32. Bakar NA, Klonis N, Hanssen E, Chan C, Tilley L. Digestive-vacuole genesis and endocytic processes in the early intraerythrocytic stages of *Plasmodium falciparum. J Cell Sci*. 2010;123:441-450; doi: 10.1242/jcs.061499.
33. Krugliak M, Zhang J, Ginsburg H. Intraerythrocytic *Plasmodium falciparum* utilizes only a fraction of the amino acids derived from the digestion of host cell cytosol for the biosynthesis of its proteins. *Mol Biochem Parasitol*. 2002;Feb;119(2):249-256.
34. Uemura T, Nakano A. Plant TGNs: dynamics and physiological functions*. Histochem Cell Biol*. 2013 Sep;140(3):341-345. doi: 10.1007/s00418-013-1116-7. Epub 2013 Jul 6.
35. Pfluger SL, Goodson HV, Moran JM, et al. Receptor for retrograde transport in the apicomplexan parasite *Toxoplasma gondii. Eukaryot Cell*. 2005;Feb 4(2):432--42.
36. Francia ME, Wicher S, Pace DA, Sullivan J, Moreno SNJ, Arrizabalaga G. A *Toxoplasma gondii* protein with homology to intracellular type Na^+/H^+ Exchangers is important for osmoregulation and invasion*. Exp Cell Res*. 2011 Jun 10;317(10):1382–1396.
37. Parussini F, Coppens I, Shah PP, Diamond SL, Carruthers VB. Cathepsin L occupies a vacuolar compartment and is a protein maturase within the endo/exocytic system of Toxoplasma gondii*. Mol Microbiol*. 2010;76(6):1340-1357.
38. Uemura T, Suda Y, Ueda T, Nakano A. Dynamic Behavior of the trans-Golgi Network in Root Tissues of Arabidopsis Revealed by Super-Resolution Live Imaging*. Plant Cell Physiol*. 2014 Apr;55(4):694-703. doi: 10.1093/pcp/pcu010. Epub 2014 Jan 18.
39. Sakura T, Sindikubwabo F, Oesterlin LK, et al. A Critical Role for *Toxoplasma gondii* Vacuolar Protein Sorting VPS9 in Secretory Organelle Biogenesis and Host Infection*. Sci Rep*. 2016 Dec 14;6:38842-doi: 10.1038/srep38842.
40. Radke JR, Striepen B, Guerini MN, Jerome ME, Roos DS, White MW. Defining the cell cycle for the tachyzoite stage of *Toxoplasma gondii. Mol Biochem Parasitol*. 2001;115(2):165-175.
41. Hu K, Johnson J, Florens L, et al. Cytoskeletal components of an invasion machine--the apical complex of *Toxoplasma gondii*. *PLoS Pathog*. 2006;Feb;2(2):e13:Epub.
42. Lebrun M, Michelin A, El Hajj H, et al. The rhoptry neck protein RON4 re-localizes at the moving junction during *Toxoplasma gondii* invasion*. Cell Microbiol*. 2005;7(12):1823-1833. doi: 10.1111/j.1462-5822.2005.00646.x.
43. Ferguson SM, De Camilli P. Dynamin, a membrane-remodelling GTPase*. Nat Rev Mol Cell Biol*. 2012;13(2):75-88. doi: 10.1038/nrm3266.
44. Fujimoto M, Tsutsumi N. Dynamin-related proteins in plant post-Golgi traffic*. Front Plant Sci*. 2014;5:408. doi: 10.3389/fpls.2014.00408.
45. Hinshaw JE. Dynamin and its role in membrane fission*. Annu Rev Cell Dev Biol*. 2000;16:483-519. doi: 10.1146/annurev.cellbio.16.1.483.
46. Smaczynska-de R,II, Allwood EG, Aghamohammadzadeh S, Hettema EH, Goldberg MW, Ayscough KR. A role for the dynamin-like protein Vps1 during endocytosis in yeast*. J Cell Sci*. 2010;123(Pt 20):3496-3506. doi: 10.1242/jcs.070508 [doi].
47. Milani KJ, Schneider TG, Taraschi TF. Defining the Morphology and Mechanism of the Hemoglobin Transport Pathway in *Plasmodium falciparum* Infected Erythrocytes*. Eukaryot Cell*. 2015. doi: EC.00267-14 [pii].
48. Damke H, Baba T, Warnock DE, Schmid SL. Induction of mutant dynamin specifically blocks endocytic coated vesicle formation*. J Cell Biol*. 1994;127(4):915-934.
49. Slomianny C. Three-dimensional reconstruction of the feeding process of the malaria parasite*. Blood Cells*. 1990;16(2-3):369-378.
50. Behnke MS, Wootton JC, Lehmann MM, et al. Coordinated progression through two subtranscriptomes underlies the tachyzoite cycle of *Toxoplasma gondii. PloS one*. 2010.
51. Nishi M, Hu K, Murray JM, Roos DS. Organellar dynamics during the cell cycle of *Toxoplasma gondii. J Cell Sci*. 2008;121(Pt 9):1559-1568. doi: 10.1242/jcs.021089.
52. Subach FV, Subach OM, Gundorov IS, et al. Monomeric fluorescent timers that change color from blue to red report on cellular trafficking. *Nat Chem Biol*. 2009 Feb;5(2):118-126.
53. Khmelinskii A, Knop M. Analysis of protein dynamics with tandem fluorescent protein timers. *Methods Mol Biol*. 2014;1174:195-210. doi: 10.1007/978-1-4939-0944-5_13.
54. Agueta F, Upadhyayulab S, Gaudinb R, et al. Membrane dynamics of dividing cells imaged by lattice light-sheet microscopy. *Mol Biol Cell*. 2016 Nov 7;27(22):3418-3435. Epub 2016 Aug 17.
55. Tacheva-Grigorova SK, Santos AJ, Boucrot E, Kirchhausen T. Clathrin-mediated endocytosis persists during unperturbed mitosis*. Cell Rep*. 2013 Aug 29;4(4):659-668. doi: 10.1016/j.celrep.2013.07.017. Epub 2013 Aug 15.
56. Fielding AB, Royle SJ. Mitotic inhibition of clathrin-mediated endocytosis*. Cell Mol Life Sci*. 2013 Sep;70(18):3423-3433. doi: 10.1007/s00018-012-1250-8. Epub 2013 Jan 11.
57. Aikawa M, Hepler PK, Huff CG, Sprinz H. The feeding mechanism of avian malarial parasites. *J Cell Biol*. 1966;Feb;28(2):355-373.

58. Gaji RY, Behnke MS, Lehmann MM, White MW, Carruthers VB. Cell cycle-dependent, intercellular transmission of *Toxoplasma gondii* is accompanied by marked changes in parasite gene expression. *Mol Microbiol*. 2011;79(1):192-204. doi: 10.1111/j.1365-2958.2010.07441.x; 10.1111/j.1365-2958.2010.07441.x.
59. Lobo CA, Rodriguez M, Hou G, Perkins M, Oskov Y, Lustigman S. Characterization of PfRhop148, a novel rhoptry protein of *Plasmodium falciparum. Mol Biochem Parasitol*. 2003 Apr 25;128(1):59-65.
60. Topolska AE, Lidgett A, Truman D, Fujioka H, Coppel RL. Characterization of a Membrane-associated Rhoptry Protein of *Plasmodium falciparum. J Biol Chem*. 2004 Feb 6;279(6):4648-4656. Epub 2003 Nov 12.
61. Renard HF, Johannes L, Morsomme P. Increasing Diversity of Biological Membrane Fission Mechanisms. *Trends Cell Biol*. 2018. doi: S0962-8924(17)30234-9 [pii].
62. Kumari S, Mayor S. ARF1 is directly involved in dynamin-independent endocytosis. *Nat Cell Biol*. 2008;10(1):30-41. doi: ncb1666 [pii].
63. Choi JH, Park JB, Bae SS, et al. Phospholipase C-gamma1 is a guanine nucleotide exchange factor for dynamin-1 and enhances dynamin-1-dependent epidermal growth factor receptor endocytosis. *J Cell Sci*. 2004;117(Pt 17):3785-3795. doi: 10.1242/jcs.01220.
64. Pucadyil TJ, Schmid SL. Conserved functions of membrane active GTPases in coated vesicle formation. *Science*. 2009;325(5945):1217-1220. doi: 10.1126/science.1171004.
65. Chaudhary N, Gomez GA, Howes MT, et al. Endocytic crosstalk: cavins, caveolins, and caveolae regulate clathrin-independent endocytosis. *PLoS Biol*. 2014;12(4):e1001832. doi: 10.1371/journal.pbio.1001832.
66. Nichols BA, Chiappino ML, Pavesio CE. Endocytosis at the micropore of Toxoplasma gondii. *Parasitol Res*. 1994;80(2):91-98.
67. Sibley LD, Niesman IR, Parmley SF, Cesbron-Delauw MF. Regulated secretion of multi-lamellar vesicles leads to formation of a tubulo-vesicular network in host-cell vacuoles occupied by Toxoplasma gondii. *J Cell Sci*. 1995;108 (Pt 4)(Pt 4):1669-1677.
68. Travier L, Mondragon R, Dubremetz JF, et al. Functional domains of the Toxoplasma GRA2 protein in the formation of the membranous nanotubular network of the parasitophorous vacuole. *Int J Parasitol*. 2008;38(7):757-773. doi: 10.1016/j.ijpara.2007.10.010.
69. Wojczyk BS, Stwora-Wojczyk MM, Hagen FK, et al. cDNA cloning and expression of UDP-N-acetyl-D-galactosamine:polypeptide N-acetylgalactosaminyltransferase T1 from *Toxoplasma gondii*. *Mol Biochem Parasitol*. 2003;131(2):93-107.
70. Zhao Y, Khaminets A, Hunn J, Howard J. Disruption of the Toxoplasma gondii parasitophorous vacuole by IFNγ-inducible immunity related GTPases (IRG proteins) triggers necrotic cell death. *PLoS Pathogens*. 2009;5(2):e1000288.
71. Larson ET, Parussini F, Huynh MH, et al. Toxoplasma gondii cathepsin L is the primary target of the invasion-inhibitory compound morpholinurea-leucyl-homophenyl-vinyl sulfone phenyl. *J Biol Chem*. 2009;284(39):26839-26850. doi: 10.1074/jbc.M109.003780.
72. Dou Z, Coppens I, Carruthers VB. Non-canonical Maturation of Two Papain-family Proteases in Toxoplasma gondii. *J Biol Chem*. 2013;288(5):3523-3534. doi: 10.1074/jbc.M112.443697; 10.1074/jbc.M112.443697.
73. Burg JL, Perlman D, Kasper LH, Ware PL, Boothroyd JC. Molecular analysis of the gene encoding the major surface antigen of *Toxoplasma gondii. J Immunol*. 1988;141:3584-3591.
74. Morris MT, Coppin A, Tomavo S, V C. Functional analysis of *Toxoplasma gondii* protease inhibitor 1. *J Biol Chem*. 2002;277(47):45259-66.
75. Achbarou A, Mercereau-Puijalon O, Autheman JM, Fortier B, Camus D, Dubremetz JF. Characterization of microneme proteins of Toxoplasma gondii. *Mol Biochem Parasitol*. 1991;47(2):223-233. doi: 0166-6851(91)90182-6 [pii].
76. Mann T, Beckers C. Characterization of the subpellicular network, a filamentous membrane skeletal component in the parasite *Toxoplasma gondii. Mol Biochem Parasitol*. 2001;115(2):257-268.
77. Kafsack BF, Beckers C, Carruthers VB. Synchronous invasion of host cells by Toxoplasma gondii. *Mol Biochem Parasitol*. 2004;136(2):309-311.
78. Huynh MH, Rabenau KE, Harper JM, Beatty WL, Sibley LD, V C. Rapid invasion of host cells by *Toxoplasma* requires secretion of the MIC2-M2AP adhesive protein complex. *Embo J*. 2003;22(9):2082-2090.

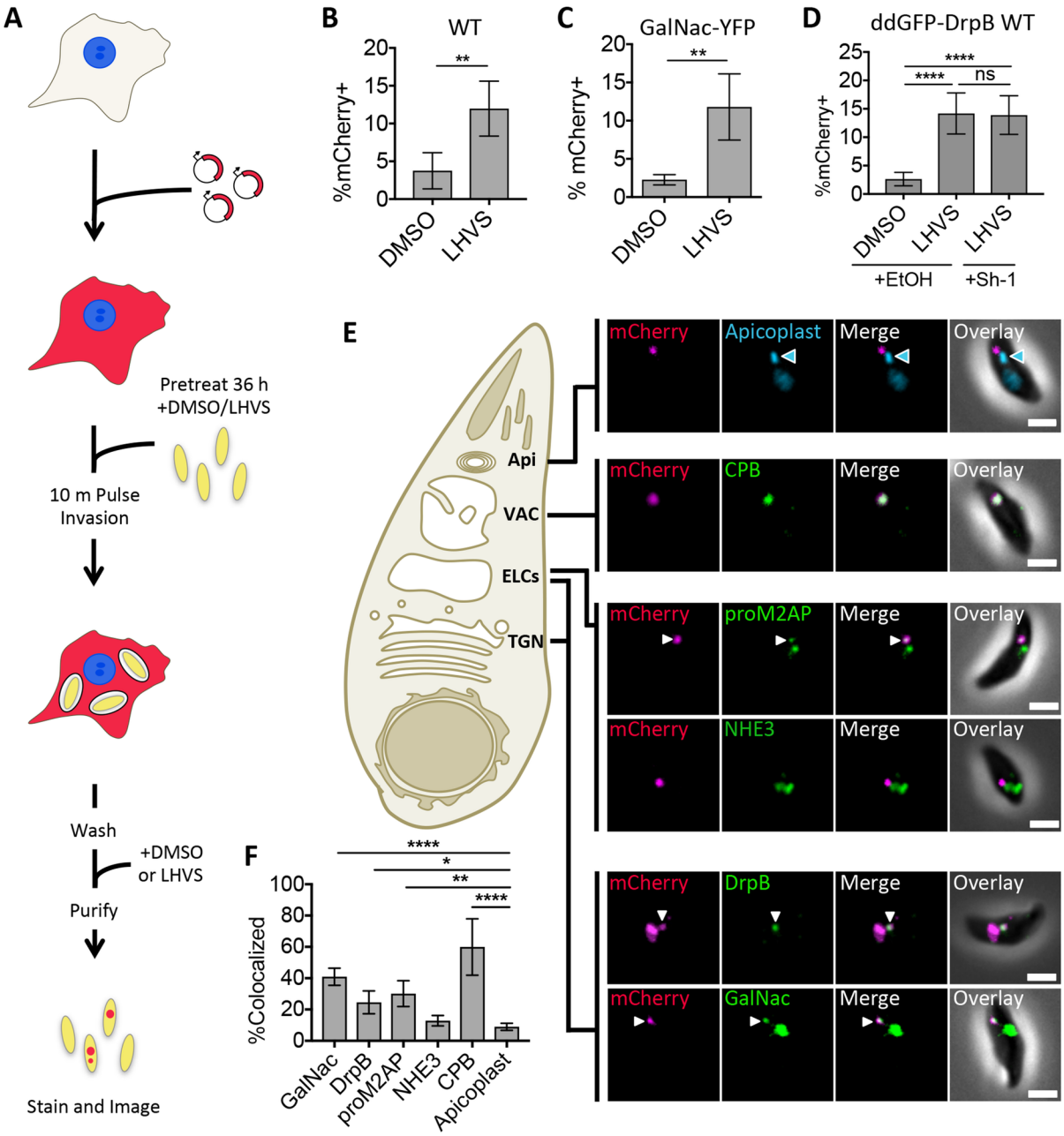

Fig1.tiff

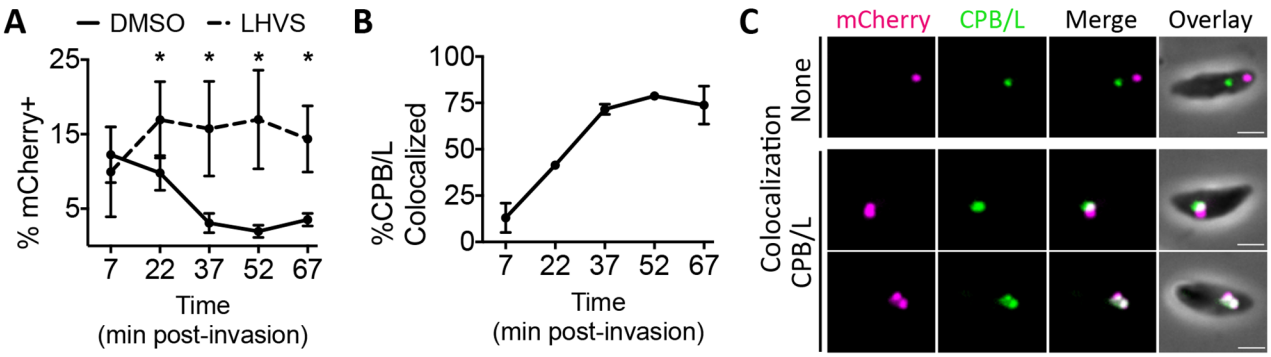

Fig2.tiff

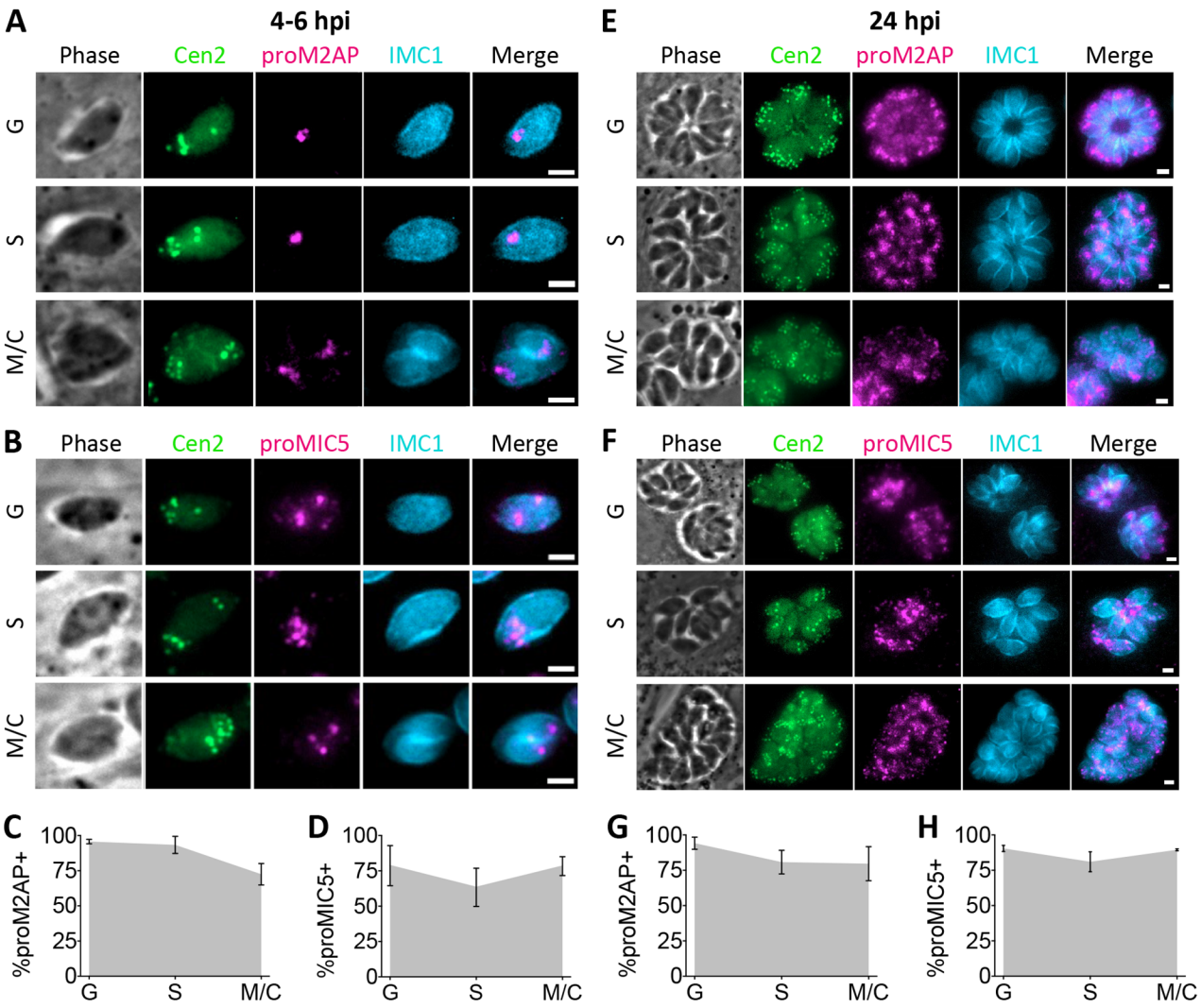

Fig3.tiff

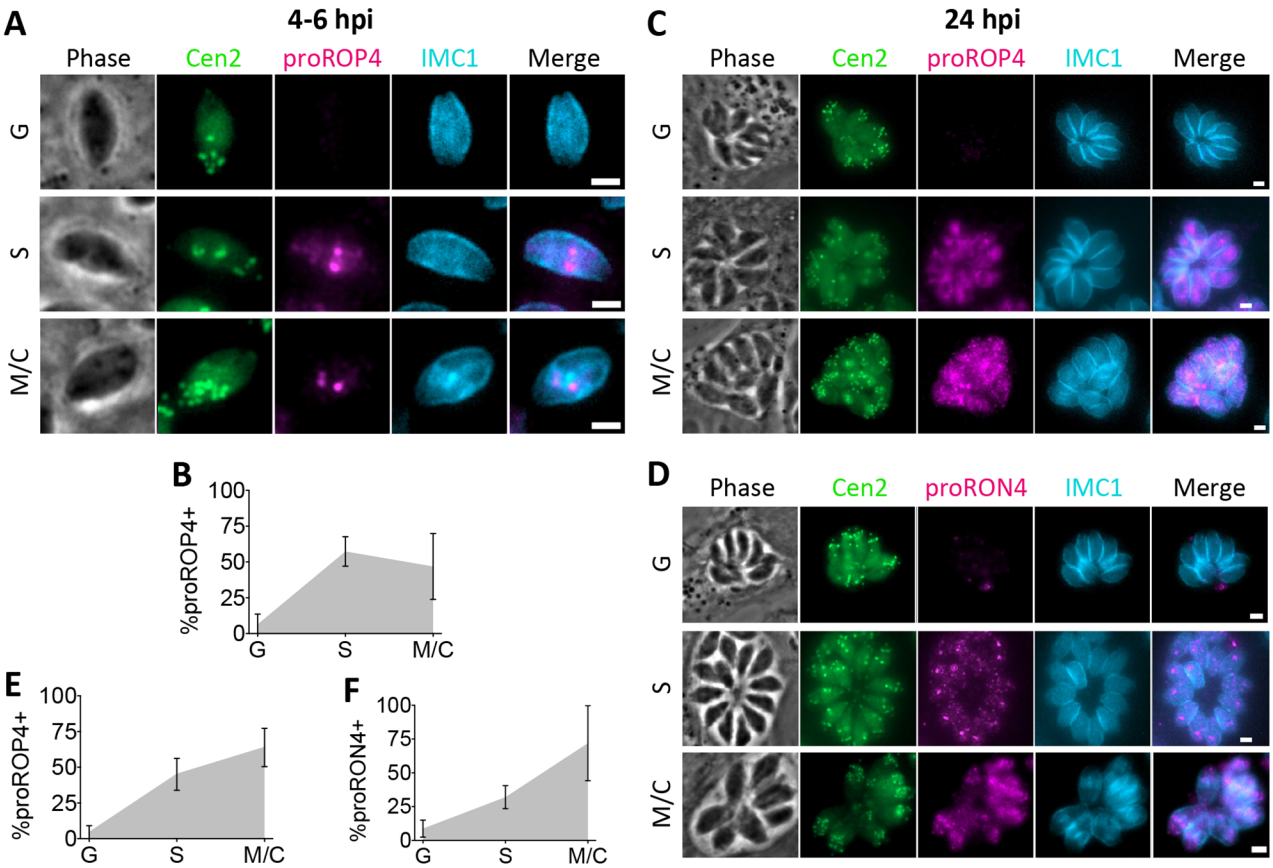

Fig4.tiff

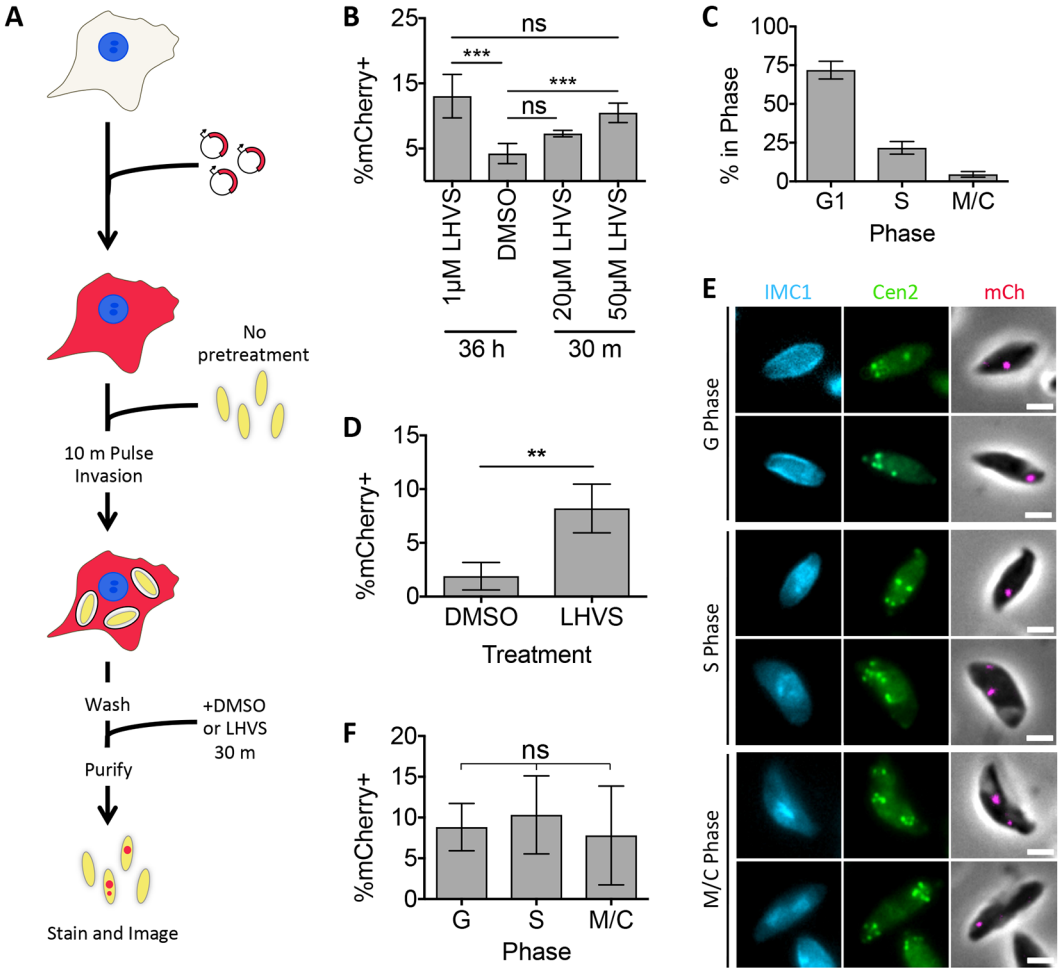

Fig5.tiff

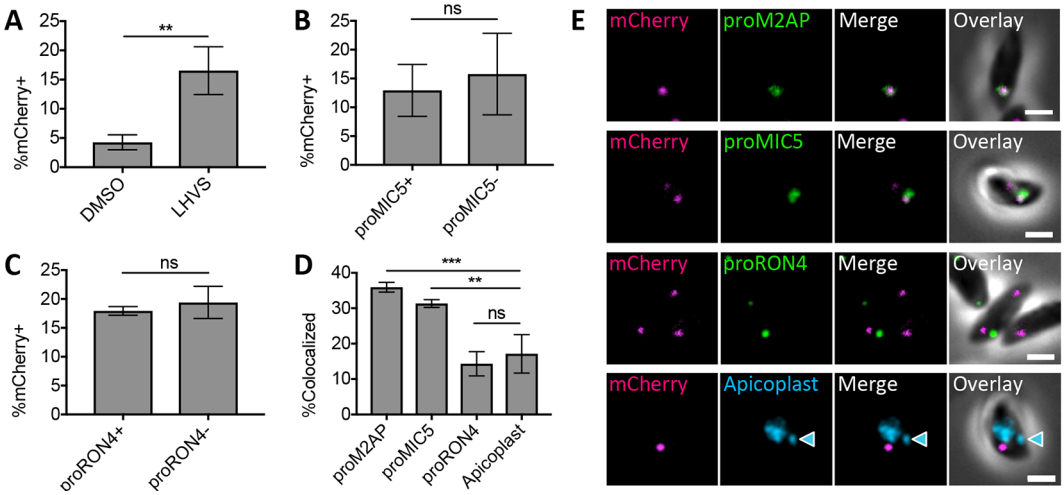

Fig6.tiff

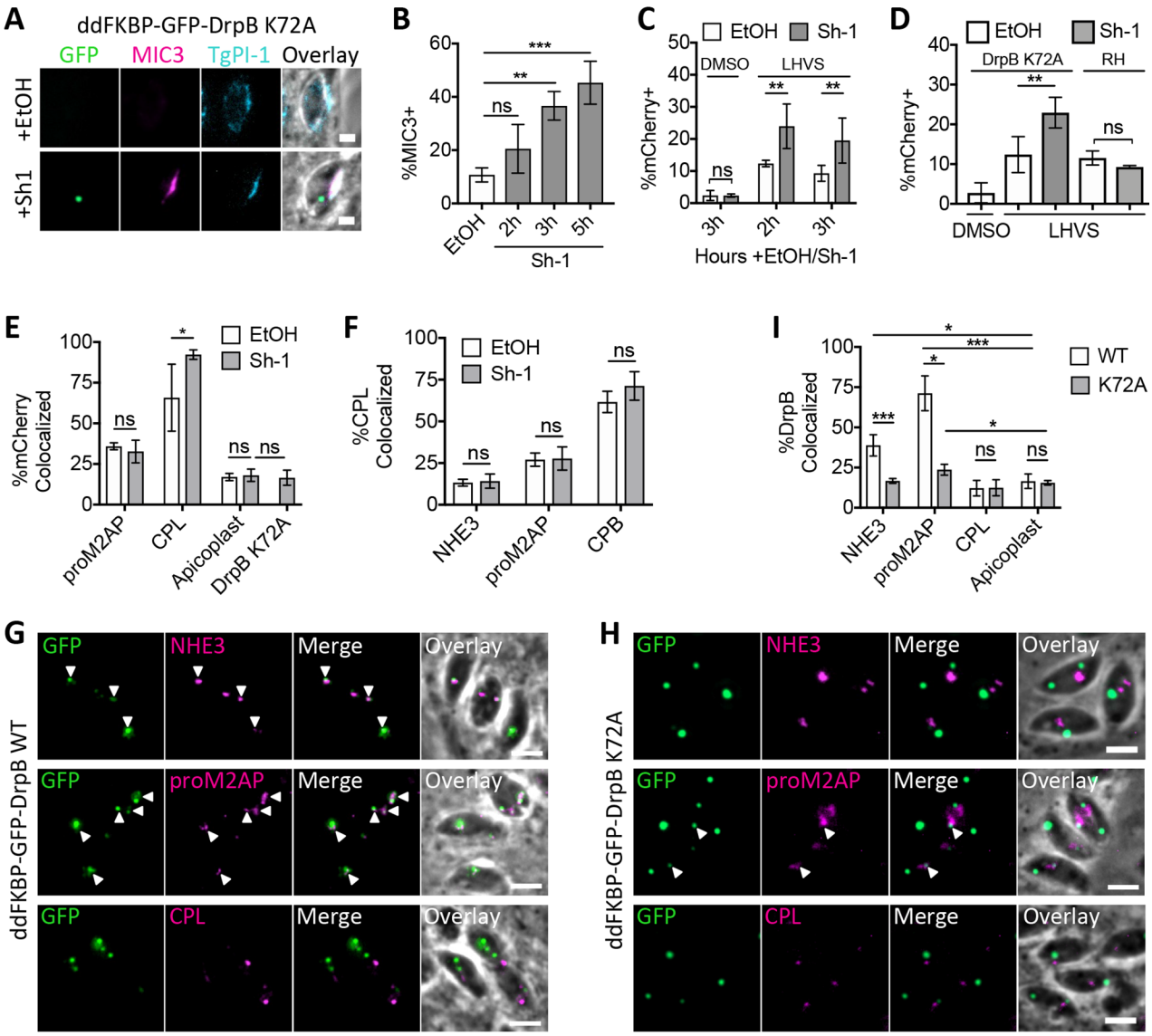

Fig7.tiff

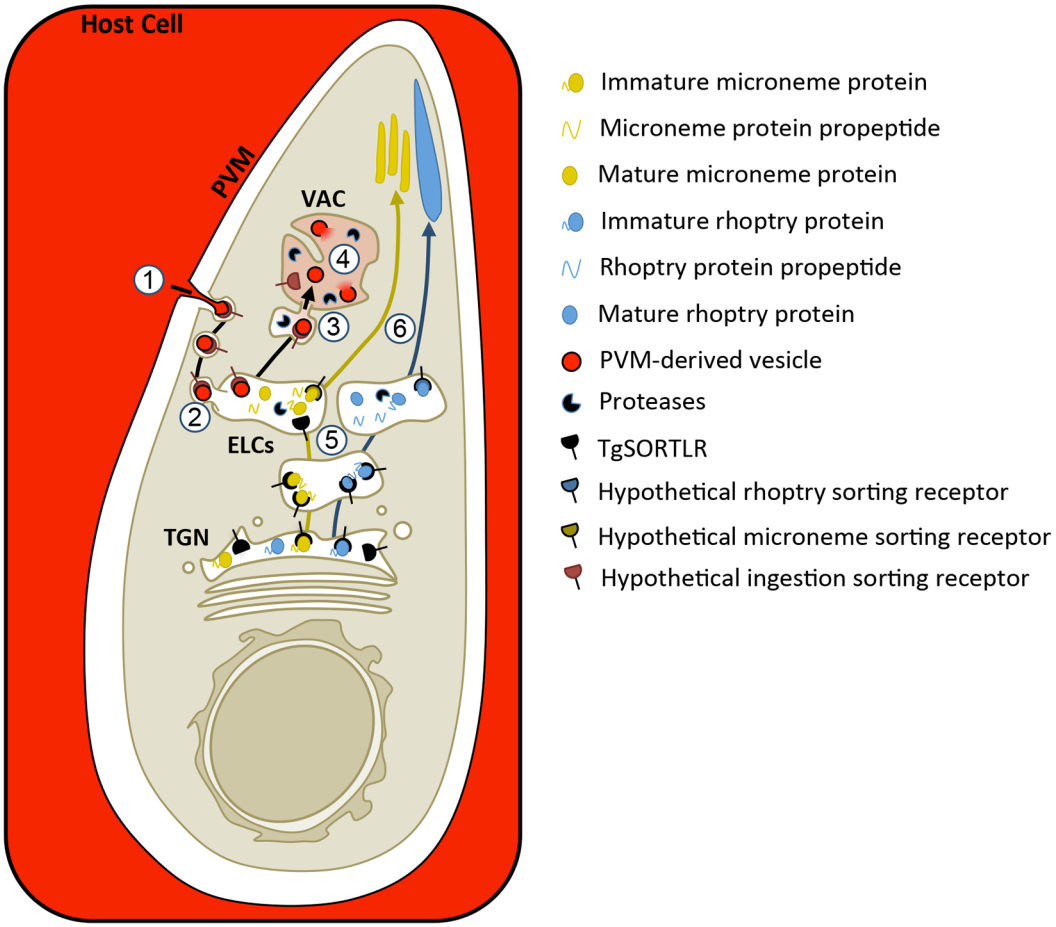

Fig8.tiff

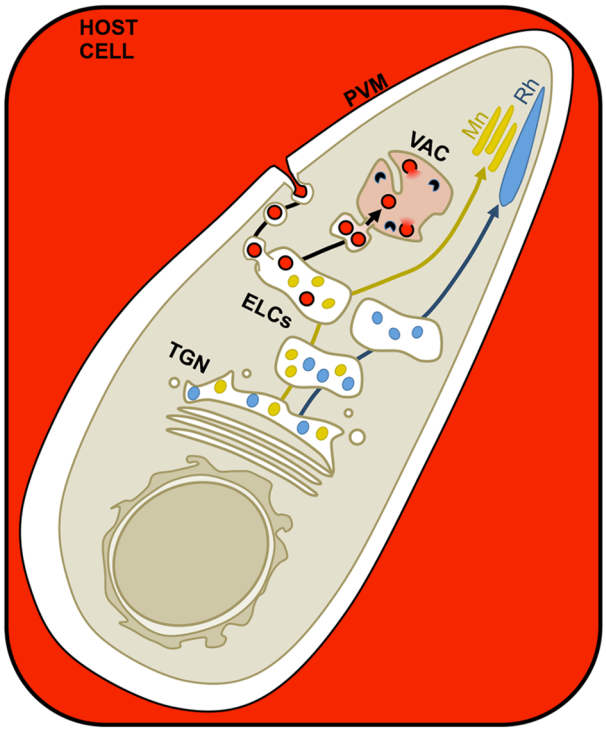

tra_12556_AbstractFigure.tif

Title:	Intersection of Endocytic and Exocytic Systems in *Toxoplasma gondii*
Authors:	Olivia L. McGovern, Yolanda Rivera-Cuevas, Geetha Kannan, Andrew Narwold Jr., and Vern B. Carruthers
Article Type:	Original Research

Monitoring Editor	Dominique Soldati-Favre
Date Submitted	20 October 2017
Date for Decision 1	4 December 2017
Date Resubmitted	18 January 2018
Date for Decision 2	4 February 2018
Accepted	10 February 2018

Decision and Reviews

Dear Dr. Carruthers, dear Vern,

Thank you for submitting your manuscript "Intersection of endocytic and exocytic systems in Toxoplasma gondii" for consideration for publication in Traffic. I asked two colleagues who are experts in the field to review the paper and their verbatim comments are appended below. I share the view of the referees that the work presented in this paper is of a high technical caliber and will be of interest. However, I also agree with both referees that some mechanistic insight (functional interference of endocytosis) would significantly increase the impact of this study. The referees have made excellent suggestions for the experiments to include.

Although I cannot accept your manuscript for publication at this point, I believe that you will be able to address the referees' concerns and I look forward to receiving your revised manuscript. To expedite handling when you resubmit please be sure to include a response outlining how you have addressed each of the referees' concerns.

Sincerely,

Dominique Soldati-Favre, Ph.D.
Associate Editor

Referee's Comments to the Authors

Referee: 1

Comments to the Author
Review of McGovern et al.,
Summary:
In this study the authors investigate the trafficking of ingested host cell proteins by the apicomplexan parasite Toxoplasma gondii. Previous studies by the Carruther's group demonstrated the intracellular parasites are capable to take up host proteins that are trafficked to a lysosome like compartment, the VAC. However, to date it is unknown, how this protein uptake occurs, which routes are taken and which trafficking factors are used.
In this study the Carruther's group demonstrate that endocytic and exocytic pathways intersect and that the host proteins are delivered to the VAC using a (probably) conserved transport pathway.
Furthermore, the authors present evidences that de novo synthesis and transport of micronemal proteins occur throughout the cell cycle, while rhoptry proteins appear to be synthesised only during S and M/C phase.
Together this study provides important novel insights about the general organisation of endocytic and exocytic transport pathways in Toxoplasma gondii

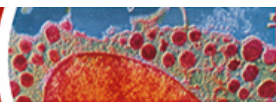

Own opinion:
The authors use a nice and reliable assay in order to detect and follow the uptake of a reporter protein (mCherry), expressed in the host cell, into the parasite. Previously the authors demonstrated uptake and delivery of the proteins into the VAC, indicating involvement of a "conserved" trafficking machinery, similar to other eukaryotes.
In general, the performed analysis is well conducted and the conclusions appear valid. I think the study is of general interest and can be published after (minor) revision.

Major criticism:
1.) The study is observational and could be substantially improved by providing some mechanism, to determine if ingestions uses (as proposed) conserved factors. This could be achieved by using some mutants for the discussed endocytic factors (Clathrin, Dynamin, etc.). Alternatively, inhibitors such as Pitstop, Phenylarsine or Cytochalasin D could be used to assess if uptake is clathrin or actin dependent.

2.) The whole experimental approach is based on end point assays followed by colocalisation analysis. Although properly done with all necessary controls provided, it would be great if the authors could provide more dynamic insights using time lapse imaging.

3.) The necessity to scratch syringe the parasite prior to image analysis is introducing some uncertainty. Did the authors test if parasites positive for mCherry are viable and can re-invade?

4.) The authors provide data concerning de novo synthesis of microneme and rhoptry proteins and reach the conclusion that micronemes are synthesised throughout the cell cycle, whereas rhoptries are only synthesised during S and M/C phase. These results are in conflict to Besterio et al, 2009 (see Figure 4). In this study the authors concluded that synthesis of micronemes and rhoptries is tightly regulated and asynchronous. Importantly, co-staining with proM2AP/proRon4 or proRon8/proMIC3 demonstrated the presence of PVs with parasites either positive for the rhoptry OR the microneme marker, indicating tight regulation of both. It might be a choice of markers and/or antibodies that leads to these differences. It is suggested to repeat the experiment to solve this issue, since it is a major point of the study.

Minor criticism:
1.) The model in Figure 5 assumes uptake via the micropore. The authors demonstrated in a previous report that the presence of the intravacuolar network is critical for uptake, suggesting that proteins enter the parasite via this network. The authors should discuss this in more detail. At this point it is still unclear how the host proteins enter the parasite.

2.) The discussion could be significantly shortened and more focused on the presented results.

Referee: 2

Comments to the Author
This manuscript provides a careful quantitative imaging-based analysis of the interaction between the newly described endocytic pathway and the better studied exocytic pathway in Toxoplasma. The data generally appears high quality, largely reproducible (although with large error bars in some cases) and is carefully controlled. The data concludes, from a battery of co-localisation experiments, that micronemal proteins and the endocytic pathway intersect, but that rhoptry proteins take a different route and are more tightly cell-cycle regulated.

Overall, I find this work solid and important to report (provided the comments below), however, this manuscript has nothing in the way of functional work to back up the claims of this proposed pathway. This is eminently achievable given available genetic tools and prior knowledge in Rab biology and characterization of molecular players in the Toxo secretory pathway. Any molecular understanding of this pathway would be very welcome and make much more compelling study.

The only major technical point that needs clarification is whether deconvolution was used throughout the study, before co-localisation was scored. This would be essential to discount co-localisation based on detection of out-of-focus light. I cannot find any evidence in the material and methods section. There is only explicit use of deconvolution in Fig S3 and associated text, making me wonder whether it was used throughout or just there?

Minor points:

In the first results section 'Characterisation of parasites stably expressing GalNAc-YFP' – no figure is referenced. I assume the authors should have referred to Figure S1 and S2?

It seems an important observation that GalNac-YFP does probably not exclusively mark the Golgi to to its co-localisation with CPL/B and mCherry. Would it be worth confirming this using the GRASP55 FP fusion?

I find it a little puzzling as to why only 5-15% of parasites (with and without LHVS) have undergone mCherry ingestion. I would have expected higher levels, over the longer periods of time assessed.

Author Rebuttal

Referee: 1
Comments to the Author
Review of McGovern et al.,
Summary:
In this study the authors investigate the trafficking of ingested host cell proteins by the apicomplexan parasite Toxoplasma gondii. Previous studies by the Carruther's group demonstrated the intracellular parasites are capable to take up host proteins that are trafficked to a lysosome like compartment, the VAC. However, to date it is unknown, how this protein uptake occurs, which routes are taken and which trafficking factors are used.
In this study the Carruther's group demonstrate that endocytic and exocytic pathways intersect and that the host proteins are delivered to the VAC using a (probably) conserved transport pathway.
Furthermore, the authors present evidences that de novo synthesis and transport of micronemal proteins occur throughout the cell cycle, while rhoptry proteins appear to be synthesised only during S and M/C phase.
Together this study provides important novel insights about the general organisation of endocytic and exocytic transport pathways in Toxoplasma gondii

Own opinion:
The authors use a nice and reliable assay in order to detect and follow the uptake of a reporter protein (mCherry), expressed in the host cell, into the parasite. Previously the authors demonstrated uptake and delivery of the proteins into the VAC, indicating involvement of a "conserved" trafficking machinery, similar to other eukaryotes.
In general, the performed analysis is well conducted and the conclusions appear valid. I think the study is of general interest and can be published after (minor) revision.

Major criticism:
1.) The study is observational and could be substantially improved by providing some mechanism, to determine if ingestions uses (as proposed) conserved factors. This could be achieved by using some mutants for the discussed endocytic factors (Clathrin, Dynamin, etc.). Alternatively, inhibitors such as Pitstop, Phenylarsine or Cytochalasin D could be used to assess if uptake is clathrin or actin dependent.

Response
This is a valid and important consideration for the study that we were aware of prior to submitting the manuscript. Accordingly, we had already started to test the role of Dynamin-related protein B (DrpB) in trafficking of ingested material using a regulatable dominant negative mutant of DrpB (ddGFP –DrpB 72A) that was previously shown to impact the trafficking of proteins to the micronemes and rhoptries. Although using a DN mutant is not without it own limitations, we felt this approach was better than using inhibitors that have not been validated in T. gondii and/or that will also have potentially confounding effects on host cells. We also carefully assessed the time-dependent effects of the DN mutant and measured impact at the shortest effective induction times to minimize secondary effects.

Interestingly, as shown in a new 9-panel figure (Figure 7), we found that interfering with DrpB function increased ingestion of host-derived protein into the parasite. The findings imply not only that ingestion does not require DrpB, but also that DrpB might restrict ingestion or that crosstalk between DrpB-dependent and DrpB-independent pathways exists. Possible explanations for these findings are also considered in the revised discussion.

Experiments are planned to test the roles of additional trafficking determinants (clathrin, rabs, adaptor proteins, etc) using the auxin-inducible degradation system, but it will take some time to optimize the system. We envision that such studies will be part of the next "chapter" in this line of investigation.

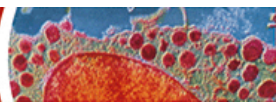

2.) The whole experimental approach is based on end point assays followed by colocalisation analysis. Although properly done with all necessary controls provided, it would be great if the authors could provide more dynamic insights using time-lapse imaging.

Response
We agree that it would be ideal to visualize ingestion via time-lapse imaging in live, infected cells. However, bright signal from the cytosol of transfected host cells obscures signal within the parasite when visualized by wide field microscopy. We attempted several strategies to obviate this. First, we tried line-scanning confocal microscopy to limit interference from out of focus signal from the host cell cytosol. Second, we used dye called pHrodo-AM, which increases in fluorescence intensity at low pH, to label the host cytosol instead of mCherry. We expected that endocytic delivery of pHrodo to the VAC should result in increased fluorescence intensity due to the acidic environment, thus allowing visualization of ingested material. Unfortunately, neither of these approaches worked sufficiently well to reliably visualize ingestion in live infected cells. We also tried expressing in the host cytosol a photoactivatable form of mCherry (PA-mCh) fused the RAH domain of TgROP5, which directs association with the PVM. This approach significantly reduced signal from the host cell by selectively photoactivating PA-mCh proximal to the PVM. We were able to visualize what appeared to be vesicular trafficking within the PV, but we were unable to track it into the parasite. We also failed to detect accumulation of TgROP5 RAH domain fused to YFP in the parasite using our traditional ingestion assay, implying that ingestion of this protein is below the limit of detection. We are currently testing a protease-activated mCherry, but have thus far not seen evidence of this working. We will continue to invest in strategies for live imaging, but a solution for this is not available presently.

3.) The necessity to scratch syringe the parasite prior to image analysis is introducing some uncertainty. Did the authors test if parasites positive for mCherry are viable and can re-invade?

Response

This is an important point that we tested by recovering LHVS treated parasites from inducible mCherry CHO host cells according to our normal harvest procedure, and inoculated them into fresh HFF cells. We found that mCherry+ parasites were capable of binding to HFF cells and a similar proportion were able to successfully invade host cells (FigureS3A-C), suggesting that mCherry+ positive parasites are viable. That this proportion is somewhat lower than the ~42% of total parasites that were mCherry+ (based on FigureS5C) is probably due to the known effect of LHVS treatment on microneme secretion, which is required for parasite attachment and invasion (Teo et al, Antimicrob Agents Chemother 2007). The ability of mCherry+ parasites to reinvade host cells is now mentioned in the first paragraph of the section titled “Ingested proteins traverse ELCs but likely not the TGN”.

4.) The authors provide data concerning de novo synthesis of microneme and rhoptry proteins and reach the conclusion that micronemes are synthesized throughout the cell cycle, whereas rhoptries are only synthesized during S and M/C phase. These results are in conflict to Besterio et al, 2009 (see Figure 4). In this study the authors concluded that synthesis of micronemes and rhoptries is tightly regulated and asynchronous. Importantly, co-staining with proM2AP/proRon4 or proRon8/proMIC3 demonstrated the presence of PVs with parasites either positive for the rhoptry OR the microneme marker, indicating tight regulation of both. It might be a choice of markers and/or antibodies that leads to these differences. It is suggested to repeat the experiment to solve this issue, since it is a major point of the study.

Response
Although we can understand why the reviewer suggests a conflict between the data in our study versus that of Besteiro et al 2009, our study did not directly test the synchronicity of microneme versus rhoptry synthesis, and the Besteiro study did not assess microneme and rhoptry biogenesis with markers of the cell cycle. Three different individuals in our lab independently obtained similar results for analysis of cell cycle dependent expression of proMICs and proROPs, and, knowing Dr. Besteiro, it can be expected that his analysis was equally thorough. Also, we have previously validated the specificity of the affinity purified anti-proM2AP antibody on Δm2ap mutant parasites. Since we used a new batch of anti-proMIC5 for the current study, we also authenticated its specificity on Δmic5 parasites. To explain the respective findings, we suggest in the discussion that microneme biogenesis could occur in multiple waves during the cell cycle with a pause during a portion of S or M/C phase for rhoptry production. See discussion section “Cell Cycle Dependence of Microneme and Rhoptry Biogenesis”.

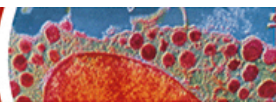

Minor criticism:
1.) The model in Figure 5 assumes uptake via the micropore. The authors demonstrated in a previous report that the presence of the intravacuolar network is critical for uptake, suggesting that proteins enter the parasite via this network. The authors should discuss this in more detail. At this point it is still unclear how the host proteins enter the parasite.

Response
These are both excellent points. Although the micropore is our best guess for the site of endocytosis in T. gondii, there is no direct evidence for this. Accordingly, we removed the micropore from the illustrated model in Figure 8. We also modified the discussion to indicate that the micropore is a likely, but not definitive site of endocytosis, based on the Plasmodium paradigm.

Discussion of the role of the IVN has also been added. As now indicated in the manuscript, Dou et al. (mBio 2014) found that ingestion was reduced in GRA2 knockout parasites, which do not have IVN tubules. This was interpreted to mean that the IVN was required for ingestion, and may contribute as a direct conduit for uptake of host cytosol. Within our model, this would mean endocytosis of IVN tubules into the parasite. However the experiment in Dou et al was performed at 24 h post-infection when GRA2 knockout leads to the loss of IVN tubules and disorganization of parasites within the PV. Our result in Figure 2 that ingestion is active at 7 min post-invasion when IVN tubules have not yet formed, suggests that the IVN is not required for acquisition of host cytosol, at least at this early time point. We have confirmed this by comparing ingestion in WT versus GRA2 knockout parasites at early time points before disorganization occurs (7 min to 3 h post-invasion), and found no significant differences. This data is not included in this paper, and will be part of the next "chapter" of our ongoing studies exploring the mechanisms of ingested protein trafficking across the PVM. With these findings, it remains possible that the IVN contributes to ingestion at later time points, or that the IVN is not directly involved in ingestion but instead affects ingestion indirectly via its role in organizing the parasites within the PV.

2.) The discussion could be significantly shortened and more focused on the presented results.

Response
We have shorted the discussion by ~22% along with placing greater emphasis on the presented results.

Additional changes to the revised manuscript:
Efforts were made to condense all sections of the manuscript. We also assessed the localization of ddGFP-DrpB WT within the T. gondii endolysosomal system (FigureS2) and colocalization of ingested host mCherry with ddGFP-DrpB DrpB (Figure 1) to compliment the data in Figure 7 addressing the role of DrpB in T. gondii endocytosis. Figures S3 and S4 were combined to accommodate a new Figure S2.

Referee: 2
Comments to the Author
This manuscript provides a careful quantitative imaging-based analysis of the interaction between the newly described endocytic pathway and the better studied exocytic pathway in Toxoplasma. The data generally appears high quality, largely reproducible (although with large error bars in some cases) and is carefully controlled. The data concludes, from a battery of co-localisation experiments, that micronemal proteins and the endocytic pathway intersect, but that rhoptry proteins take a different route and are more tightly cell-cycle regulated.

1.) Overall, I find this work solid and important to report (provided the comments below), however, this manuscript has nothing in the way of functional work to back up the claims of this proposed pathway. This is eminently achievable given available genetic tools and prior knowledge in Rab biology and characterization of molecular players in the Toxo secretory pathway. Any molecular understanding of this pathway would be very welcome and make much more compelling study.

Response
Since this a similar comment was provided by R1, we reiterate the response as follows:

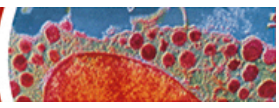

This is a valid and important consideration for the study that we were aware of prior to submitting the manuscript. Accordingly, we had already started to test the role of Dynamin-related protein B (DrpB) in trafficking of ingested material using a regulatable dominant negative mutant of DrpB (ddGFP –DrpB 72A) that was previously shown to impact the trafficking of proteins to the micronemes and rhoptries. Although using a DN mutant is not without it own limitations, we felt this approach was better than using inhibitors that have not been validated in T. gondii and/or that will also have potentially confounding effects on host cells. We also carefully assessed the time-dependent effects of the DN mutant and measured impact at the shortest effective induction times to minimize secondary effects.

Interestingly, as shown in a new 9-panel figure (Figure 7), we found that interfering with DrpB function increased ingestion of host-derived protein into the parasite. The findings imply not only that ingestion does not require DrpB, but also that DrpB might restrict ingestion or that crosstalk between DrpB-dependent and DrpB-independent pathways exists. Possible explanations for these findings are also considered in the revised discussion.

Experiments are planned to test the roles of additional trafficking determinants (clathrin, rabs, adaptor proteins, etc) using the auxin-inducible degradation system, but it will take some time to optimize the system. We envision that such studies will be part of the next "chapter" in this line of investigation.

2.) The only major technical point that needs clarification is whether deconvolution was used throughout the study, before co-localisation was scored. This would be essential to discount co-localisation based on detection of out-of-focus light. I cannot find any evidence in the material and methods section. There is only explicit use of deconvolution in FigureS3 and associated text, making me wonder whether it was used throughout or just there?

Response
Deconvolution was used for FigureS4, but it was not used for colocalization studies because we do not have access to a fast deconvolution instrument capable of rapidly capturing the Z-stacks needed for accurate deconvolution on large enough image sets to obtain robust quantitative data. We understand that wide field microscopy has limitations; however, it should be noted that ingested material did not substantially colocalize with all discrete apical markers including the apicoplast or NHE3, providing a measure of validity to the more obvious colocalization seen with proM2AP, CPB, and DrpB (Figure1). We expect that our future work will take advantage of major instrumentation upgrades that are pending at our host institution to achieve greater resolution and thus more precise localization analysis.

Minor points:

1.) In the first results section 'Characterization of parasites stably expressing GalNAc-YFP' – no figure is referenced. I assume the authors should have referred to Figure S1 and S2?

Response
Reference to FigureS1 was inserted into this section.

2.) It seems an important observation that GalNac-YFP does probably not exclusively mark the Golgi to its co-localisation with CPL/B and mCherry. Would it be worth confirming this using the GRASP55 FP fusion?

Response
Thank you for this suggestion. Please see FigureS1 where images comparing GalNac-YFP and GRASP55-RFP are included. In the bottom panel, a new image, which has clearer GRASP55-free signal, has been substituted and white arrowheads indicate the Golgi-free bodies. Please find a description of the colocalization of GalNac-YFP and GRAS55-RFP including a more explicit statement about GalNac-YFP not being restricted to the TGN included in the text results section now titled "Localization of TGN/ELC markers: GalNac and DrpB" and summarized below:

"Consistent with TGN localization, GalNac-YFP appeared in a centrally located structure that overlapped substantially with, or was just apical to, the Golgi marker GRASP55-mRFP (Figure S1). As previously observed, GalNac-YFP sometimes showed a high degree of overlap with another TGN marker the dynamin-related protein DrpB (Figure S1A top panel), but in other cases showed partial or no overlap with DrpB (Figure S1A bottom panel). Interestingly, GalNac-YFP overlapped best with NHE3 in the central region of the parasite despite previous observations that NHE3 partially colocalized with the VAC.36 Therefore, we interpret NHE3 to be an ELC marker that partially overlaps with the TGN, similar to the established ELC marker proM2AP.10,37 GalNac-YFP also partially overlapped with proM2AP,

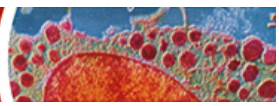

but rarely colocalized with the VAC markers CPB and CPL or the apicoplast. We also observed that some parasites had GalNac-YFP-labeled structures that were not associated with GRASP55-mRFP (Figure S1, white arrowheads). These structures are reminiscent of "Golgi-free" TGN bodies in plants38 This observation together with substantial overlap with the ELC marker proM2AP, suggests GalNac-YFP occupies the TGN, ELCs, and perhaps additional sites."

3.) I find it a little puzzling as to why only 5-15% of parasites (with and without LHVS) have undergone mCherry ingestion. I would have expected higher levels, over the longer periods of time assessed.

Response
Thank you for the opportunity to explain the apparent low percentage of mCherry+ parasites. LHVS treated parasites recovered from transiently transfected CHO host cells are 10-15% mCherry+. Since only 20% of transiently transfected host cells are mCherry+ (FigureS5B), this means that 50-75% of the parasites exposed to mCherry have ingested mCherry. LHVS treated parasites recovered from inducible mCherry CHO cells are ~42% mCherry positive (FigureS5C). Because approximately 76% of inducible mCherry CHO cells are mCherry+, this indicates that roughly 55% of the parasites exposed to mCherry have ingested this reporter. Together this suggests that most parasites are actively endocytosing material from the host cytosol. It is possible that this is an underestimate for several reasons: (1) some of the transiently transfected mCherry+ host cells are dimmer than others; hence ingestion from these cells might not reach the threshold of detection within the parasite by microscopy; (2) although more uniform in expression, the inducible mCherry CHO cells are generally dimmer than the brightest transiently transfected cells (FigureS5), thus less active parasites might not accumulate sufficient mCherry for detection; (3) LHVS treatment inactivates CPL and probably CPB, but does not inactivate other yet-to-be-identified VAC proteases that are responsible for residual proteolytic activity in the VAC (Dou et al., mBio 2014). Accordingly ingested mCherry is still being turned over to some extent in LHVS treated parasites, further limiting detection in some parasites; and (4) although mCherry is more pH tolerant than e.g., GFP, the low pH of the VAC could compromise the signal in less parasites that are less trophic. To summarize, we do not know precisely what proportion of the parasites are actively endocytosing material from the host cytosol, but the available evidence suggests it is at least half of the population.

Additional changes to the revised manuscript:
Efforts were made to condense all sections of the manuscript. We also assessed the localization of ddGFP-DrpB WT within the T. gondii endolysosomal system (FigureS2) and colocalization of ingested host mCherry with ddGFP-DrpB DrpB (Figure 1) to compliment the data in Figure 7 addressing the role of DrpB in T. gondii endocytosis. Figures S3 and S4 were combined to accommodate a new Figure S2.

Decision and Reviews

Dear Dr. Carruthers, dear Vern,

Thank you for submitting your revised manuscript "Intersection of endocytic and exocytic systems in Toxoplasma gondii" to Traffic. I asked the referees to read the paper and their verbatim comments are appended below. I agree with the referees that you have adequately addressed the concerns raised previously and I am pleased to accept this paper for publication.

Sincerely,

Dominique Soldati-Favre, PhD
Associate Editor

Referee's Comments to the Authors

Referee: 2

Comments to the Author
I still find it a little disappointing that the authors have only included, what can only really be considered a negative result, as functional data. It can only be concluded here that DrpB is not involved directly in endocytosis. The authors say that more functional data is now being generated, but this will of course take much longer to analyse.

All other queries have been sufficiently addressed.

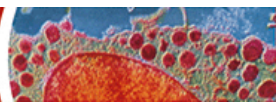

Referee: 1

Comments to the Author
In their revision, McGovern et al. addressed all my initial concerns. While the results regarding DrpB are not demonstrating a potential mechanisms for endocytic uptake and are somewhat confusing, the authors discuss these findings appropriately. It is out of the scope of this study to characterise additional, potential trafficking factors involved in endocytosis. As it stands, this would likely result in a huge fishing approach and would not be feasible within a realistic revision time.
Meanwhile, this study clearly demonstrates uptake via a "partially" conserved endocytic/exocytic transport system in Toxoplasma gondii and will be of general interest to the field.
I congratulate the authors to a nice and well performed study.

Traffic